

University of Alabama in Huntsville

**LOUIS**

---

Theses

UAH Electronic Theses and Dissertations

---

2024

## **Adaptive sliding mode control for plants with unknown parameters with adaptive boundary layer thickness for chatter attenuation**

Josiah Schlabach

Follow this and additional works at: <https://louis.uah.edu/uah-theses>

---

### **Recommended Citation**

Schlabach, Josiah, "Adaptive sliding mode control for plants with unknown parameters with adaptive boundary layer thickness for chatter attenuation" (2024). *Theses*. 681.  
<https://louis.uah.edu/uah-theses/681>

This Thesis is brought to you for free and open access by the UAH Electronic Theses and Dissertations at LOUIS. It has been accepted for inclusion in Theses by an authorized administrator of LOUIS.

**ADAPTIVE SLIDING MODE CONTROL FOR  
PLANTS WITH UNKNOWN PARAMETERS  
WITH ADAPTIVE BOUNDARY LAYER  
THICKNESS FOR CHATTER  
ATTENUATION**

**Josiah Schlabach**

**A THESIS**

**Submitted in partial fulfillment of the requirements  
for the degree of Master of Science in Engineering  
in  
The Department of Mechanical and Aerospace Engineering  
to  
The Graduate School  
of  
The University of Alabama in Huntsville  
August 2024**

**Approved by:**

Dr. Farbod Fahimi, Research Advisor/Committee Chair  
Dr. Avimanyu Sahoo, Committee Member  
Dr. Howard Chen, Committee Member  
Dr. George Nelson, Department Chair  
Dr. Shankar Mahalingam, College Dean  
Dr. Jon Hakkila, Graduate Dean

## **Abstract**

# **ADAPTIVE SLIDING MODE CONTROL FOR PLANTS WITH UNKNOWN PARAMETERS WITH ADAPTIVE BOUNDARY LAYER THICKNESS FOR CHATTER ATTENUATION**

**Josiah Schlabach**

**A thesis submitted in partial fulfillment of the requirements  
for the degree of Master of Science in Engineering**

**Mechanical and Aerospace Engineering**

**The University of Alabama in Huntsville**

**August 2024**

This thesis presents the development of an adaptive boundary layer sliding mode control (SMC) methodology tailored for plants with unknown parameters. The primary challenge addressed is the mitigation of chattering while ensuring robust performance in systems subject to high disturbances and parameter uncertainties. The research introduces a control law that combines existing work that dynamically adjusts the boundary layer thickness with existing work that uses adaptive laws to estimate unknown plant parameters. The stability of the proposed controller is validated with Lyapunov analysis. Simulation results demonstrate the effectiveness of the adaptive boundary layer SMC in producing good tracking control in the presence of high disturbance and unknown plant parameters.



## Acknowledgements

I would like to express my sincere gratitude to God for providing the strength and guidance needed to complete this thesis.

Deep appreciation is extended to Dr. Farbod Fahimi, my advisor, for his guidance, support, and insightful feedback throughout this process. His expertise and encouragement have been invaluable.

I would also like to thank my committee members, Dr. Avimanyu Sahoo and Dr. Howard Chen. Dr. Sahoo's knowledge of control systems and Lyapunov analysis imparted through several classes have been crucial to this work.

The support and contributions of all mentioned have been instrumental in the completion of this thesis.

# Table of Contents

<b>Abstract</b> . . . . .	<b>ii</b>
<b>Acknowledgements</b> . . . . .	<b>iv</b>
<b>Table of Contents</b> . . . . .	<b>vii</b>
<b>List of Figures</b> . . . . .	<b>viii</b>
<b>List of Tables</b> . . . . .	<b>ix</b>
<b>Chapter 1. Introduction</b> . . . . .	<b>1</b>
<b>Chapter 2. Constant Boundary Layer Sliding Mode Controller for a Plant with Uncertain Parameters</b> . . . . .	<b>5</b>
2.1 SMC with No Boundary Layer for a Plant with Known Param- eters . . . . .	5
2.1.1 Problem Statement . . . . .	5
2.1.2 Definitions of the Errors . . . . .	6
2.1.3 The Proposed Controller and the Proof of Stability . . . . .	7
2.2 Case of a Plant with Uncertain Parameters . . . . .	9
2.2.1 Bounds on Uncertain Parameters . . . . .	10

2.2.2	Control Law for the Plant with Uncertain Parameters . . . . .	11
2.3	Control Law with a Boundary Layer . . . . .	14
2.4	Simulation . . . . .	17
2.4.1	Definition of Values . . . . .	18
2.4.2	Simulation Results . . . . .	20
 <b>Chapter 3. Adaptive Boundary Layer Sliding Mode Controller for a Plant with Uncertain Parameters . . . . .</b>		<b>24</b>
3.1	Problem Statement and Control Law . . . . .	25
3.1.1	Plant Model . . . . .	25
3.1.2	Bounds on Uncertain Parameters . . . . .	27
3.1.3	Control Law . . . . .	28
3.2	Required Error Behavior for Varying Boundary Layer . . . . .	28
3.3	Control Law for Varying Boundary Layer . . . . .	30
3.3.1	Outside the Boundary Layer . . . . .	30
3.3.2	Deriving the Boundary Layer Adaptation Law . . . . .	32
3.3.3	Steady-State Boundary Layer Thickness . . . . .	35
3.3.4	Steady-state $s$ inside the Boundary Layer . . . . .	36
3.4	Simulation . . . . .	40

<b>Chapter 4. Adaptive Boundary Layer Sliding Mode Controller for a Plant with Unknown Parameters . . . . .</b>	<b>44</b>
4.1 Problem Statement . . . . .	44
4.2 Error Behavior . . . . .	46
4.3 Constant Boundary Layer . . . . .	48
4.4 Time-Varying Boundary Layer . . . . .	51
4.4.1 Required Error Behavior for Varying Boundary Layer .	51
4.4.2 Derivation of the Control Law . . . . .	52
4.4.3 Derivation of the Boundary Layer Adaptation Law . .	55
4.5 Simulation . . . . .	57
<b>Chapter 5. Conclusion . . . . .</b>	<b>64</b>
<b>References . . . . .</b>	<b>67</b>

## List of Figures

2.1	Block diagram of control law implementation . . . . .	18
2.2	Actual and desired system state vs time . . . . .	20
2.3	Control input vs time . . . . .	21
2.4	Combined error vs time . . . . .	21
2.5	Combined error vs time . . . . .	22
2.6	State error vs time . . . . .	22
3.1	Block diagram of control law implementation . . . . .	40
3.2	Actual and desired system state vs time . . . . .	41
3.3	Control input vs time . . . . .	42
3.4	Combined error vs time . . . . .	42
3.5	State error vs time . . . . .	43
4.1	Block diagram of control law implementation . . . . .	58
4.2	Actual and desired system state vs time . . . . .	59
4.3	Control input vs time . . . . .	60
4.4	Control input vs time . . . . .	60
4.5	Control input vs time . . . . .	61
4.6	Combined error vs time . . . . .	61
4.7	State error vs time . . . . .	62
4.8	Residual rho vs time . . . . .	62

## List of Tables

1.1	Chapter organization: SMC methods. . . . .	3
2.1	System functions with actual and estimated parameters. . . . .	19
2.2	Initial conditions and control parameters. . . . .	19
2.3	Combined and state errors. . . . .	23
3.1	Initial conditions and control parameters. . . . .	41
3.2	Combined and state errors. . . . .	43
4.1	Control parameters and initial state for both cases. . . . .	57
4.2	Initial system parameter estimates and adaptation law gain values. . . . .	59
4.3	Combined and state errors. . . . .	63
5.1	SMC methods: combined and state errors. . . . .	65
5.2	SMC methods: benefits and drawbacks. . . . .	66

## Chapter 1. Introduction

The Sliding Mode Control (SMC) method is often used in a variety of control problems when a robust controller is needed such as plants affected by uncertainties, disturbances, and variations in parameters. This method consists of defining a sliding surface and using a discontinuous control law to drive the plant to the sliding surface where it is confined to drive the system errors to zero [1, 2]. A common problem with SMC controllers is chattering which refers to the tendency of the control signal to oscillate at a very high frequency once the plant is near the sliding surface [3, 4]. This can cause problems with real systems when the physical components of the system cannot handle the high-frequency oscillations [5, 6, 7]. The chattering is caused by the system overshooting the sliding surface which triggers the switching function to push it back onto the sliding surface. This problem has been addressed in multiple ways [6, 8, 9, 10]. A common method is introducing a constant boundary layer to the control law and replacing the switching function with a smoother function within the boundary layer [11, 12, 13]. In other words, the controller is modified to slow down the system's convergence once it is within the boundary layer. While effective in low disturbance scenarios, this method fails under high disturbance [14]. If the boundary layer is too small, the chattering behaviour could be unaffected or only

partially attenuated; but, if it is too large, the convergence to the sliding surface is unnecessarily slowed down so the boundary layer thickness must be tuned. An adaptive boundary layer offers a solution by adjusting to suppress chattering even in the presence of high disturbance [14, 15, 16].

Another technique to mitigate chattering is higher-order SMC methods such as twisting control or fractional-order SMC, which involves taking higher-order time derivatives of the sliding surface to ensure it reaches zero. However, this method has drawbacks, including a dependency on accurately known initial conditions and an increase in chattering under disturbance compared to conventional sliding mode control [17, 18]. Additionally, it requires higher-order state derivatives such as acceleration or jerk for feedback. Using the higher-order derivatives in the feedback can be detrimental to the controller behaviour because of sensor noise [19, 20]. Observer-based sliding mode control, which introduces observers to complement the controller, has also been used in some cases. One example is the disturbance observer-based SMC which attempts to measure disturbances but is only successful for some types of disturbance [21]. Additionally, observer-based SMC can cause the control system to be less robust with respect to plant uncertainties [3].

The adaptive SMC method is an extension of the conventional SMC that has often been used for plants with uncertain or varying parameters. Adaptive SMC uses adaptive laws to estimate parameters when some parameters in the plant model are varying or otherwise unknown. This allows the engineer to skip any system identification step which would commonly be used to determine the

unknown parameters [22]. Furthermore, the adaptive laws for the parameters address the problem of plant uncertainties very well. If this can be combined with an adaptive boundary layer which deals with high disturbances well, then the resulting SMC method should be quite useful for attenuating chatter in high disturbance situations with unknown plant parameters.

In this thesis a controller will be derived that combines an adaptive SMC with an adaptive boundary layer. This will be done in several steps. As seen in Table 1.1, chapter 2 presents an SMC method with a constant boundary layer which will need manual tuning for a system with uncertain parameters that have known bounds. Chapter 3 introduces an adaptive boundary layer to the method

**Table 1.1:** Chapter organization: SMC methods.

	Chapter 2	Chapter 3	Chapter 4
Boundary Layer	Constant	Adaptive	Adaptive
System Parameters	Known Bounds	Known Bounds	Unknown
BL Tuning	Manual	Adaptive	Adaptive

from chapter 2. Both of these chapters primarily reformulate previous work of other authors [14] in the notation used in this thesis. This provides a basis of comparison for the method in chapter 4. Chapter 4, the main contribution of this thesis to existing work, presents an SMC method that uses both the adaptive

boundary layer presented in chapter 3 and adaptive laws for unknown parameters. The stability and successful tracking control of this controller will be validated by a series of proofs, primarily utilizing Lyapunov analysis. Additionally, the controller will be applied to a generic system in simulations to further demonstrate its performance and value in tracking control and to compare it to the SMC methods from chapters 2 and 3.

## **Chapter 2. Constant Boundary Layer Sliding Mode Controller for a Plant with Uncertain Parameters**

The goal of this chapter is to derive a Sliding Mode Control (SMC) method with a constant boundary layer for a plant in which uncertain parameters are bounded by known values. This goal is achieved in three consecutive stages. In section 2.1, as the first stage, an SMC controller with no boundary layer is proposed for the case in which the plant parameters are known. In section 2.2, as the second stage, an SMC controller with no boundary layer is proposed for the case in which the plant parameters are uncertain. As the third stage, the SMC control law proposed in section 2.2 is modified in section 2.3 to add a constant boundary layer to address chattering behavior in the plant response.

### **2.1 SMC with No Boundary Layer for a Plant with Known Parameters**

#### **2.1.1 Problem Statement**

In this section, an SMC control law is derived that assumes full knowledge of all the plant parameters. The plant to be analyzed is a  $n$ -th order system

modeled by the equation:

$$y^{(n)} + \sum_{i=1}^n \alpha_i f_i = bu + \delta, \quad (2.1)$$

where  $y^{(i)}$  ( $i = 0, \dots, n - 1$ ) are the states of the plant,  $u$  is the control input,  $\delta$  is the disturbance to the plant, and the  $f_i$  are known nonlinear functions of the system states. The parameters  $\alpha_i$  and  $b$  are the true plant parameters in the above equation and are assumed to be known. To simplify some of the derivations in this chapter, the following variables are defined and substituted when appropriate:

$$h = 1/b, \quad a_i = \frac{\alpha_i}{b}, \quad d = -\delta/b. \quad (2.2)$$

By rearranging the plant dynamics to isolate the input, we obtain the equation

$$hy^{(n)} + \sum_{i=1}^n a_i f_i + d = u. \quad (2.3)$$

### 2.1.2 Definitions of the Errors

The state error for the system is defined as

$$e = y - y_d, \quad (2.4)$$

where  $y_d$  is the desired output. The error dynamics are then

$$e^{(n-1)} = y^{(n-1)} - y_d^{(n-1)}. \quad (2.5)$$

This is then used to define the combined error as

$$s = e^{(n-1)} + \sum_{i=0}^{n-2} \binom{n-1}{i} \lambda^{n-i-1} e^{(i)}. \quad (2.6)$$

The above equation guarantees that if  $s$  vanishes, then the state error  $e$  exponentially approaches 0 for any positive  $\lambda$ . To obtain a more concise notation, the reference value  $y_r^{(n)}$  is defined as:

$$y_r^{(n)} = y_d^{(n)} - \sum_{i=0}^{n-2} \binom{n-1}{i} \lambda^{n-i-1} e^{(i+1)}. \quad (2.7)$$

Taking the derivative of the combined error equation (2.6) and substituting the above equation into the result gives the equation for the combined error dynamics:

$$\dot{s} = y^{(n)} - y_r^{(n)}. \quad (2.8)$$

By rearranging equation (2.3) for  $y^{(n)}$  and substituting it into the above equation, we get

$$\dot{s} = \frac{1}{h} \left( u - \sum_{i=1}^n a_i f_i - d \right) - y_r^{(n)}. \quad (2.9)$$

### 2.1.3 The Proposed Controller and the Proof of Stability

The following control law is proposed:

$$u = h y_r^{(n)} - k \operatorname{sgn}(s) + \sum_{i=1}^n a_i f_i, \quad (2.10)$$

where  $k$  has the same sign as  $h$ .

*Theorem:* If the proposed controller in equation (2.10) is applied to the plant in equation (2.3), the combined error  $s$  as defined in equation (2.6) approaches zero in a finite time, causing the error  $e$  to exponentially approach zero provided that:

$$k = \eta + D, \quad (2.11)$$

where  $\eta > 0$  and  $D \geq |\delta|$  is the bound of the disturbance.

*Proof:* Consider the positive definite Lyapunov function as follows:

$$V = \frac{1}{2}hs^2. \quad (2.12)$$

The time derivative of this Lyapunov function is

$$\dot{V} = hs\dot{s}. \quad (2.13)$$

Then substituting equation (2.9), we get:

$$\dot{V} = hs\left(\frac{1}{h}\left(u - \sum_{i=1}^n a_i f_i - d\right) - y_r^{(n)}\right). \quad (2.14)$$

Substituting the control law from equation (2.10) leads to

$$\dot{V} = hs\left(\frac{1}{h}\left(hy_r^{(n)} - k\text{sgn}(s) + \sum_{i=1}^n a_i f_i - \sum_{i=1}^n a_i f_i - d\right) - y_r^{(n)}\right). \quad (2.15)$$

Most of the terms cancel out leaving only:

$$\dot{V} = -k|s| - ds. \quad (2.16)$$

Assuming a bounded disturbance, we have  $D \geq |d|$ , so converting the above equation to an inequality gives:

$$\dot{V} \leq -k|s| + D|s|. \quad (2.17)$$

Using the chosen  $k$  from equation (2.11) reduces the above equation to

$$\dot{V} \leq -\eta|s|. \quad (2.18)$$

Because  $\dot{V}$  is always negative for all  $s$ ,  $V$  will decrease until  $|s| = 0$ , at which point the state error  $e$  will approach zero according to equation (2.6). This concludes the proof of the theorem.

## 2.2 Case of a Plant with Uncertain Parameters

The true plant is defined in equation (2.3). Here, the case where the parameters  $a_i$  and  $h$  are uncertain is considered. Since the parameters  $a_i$  and  $h$  are uncertain, the control law in equation (2.10) is not implementable. The plant equation needs to be modified to use the nominal parameters  $\hat{a}_i$  and  $\hat{h}$  shown in

the nominal plant below:

$$\hat{h}y^{(n)} + \sum_{i=1}^n \hat{a}_i f_i + d = u. \quad (2.19)$$

### 2.2.1 Bounds on Uncertain Parameters

In the nominal system,  $\hat{a}_i$  and  $\hat{h}$  are the estimates of  $a_i$  and  $h$ . These estimates are bounded by known values. The parameter  $h$  is bounded as

$$0 < h_{\min} \leq h \leq h_{\max}. \quad (2.20)$$

If  $\hat{h}$  is defined as  $\hat{h} = \sqrt{h_{\max}h_{\min}}$ , then

$$0 < \frac{h_{\min}}{\hat{h}} \leq \frac{h}{\hat{h}} \leq \frac{h_{\max}}{\hat{h}}, \quad (2.21)$$

which leads to

$$0 < \frac{h_{\min}}{\sqrt{h_{\max}h_{\min}}} \leq \frac{h}{\hat{h}} \leq \frac{h_{\max}}{\sqrt{h_{\max}h_{\min}}}. \quad (2.22)$$

This reduces algebraically to

$$\sqrt{\frac{h_{\min}}{h_{\max}}} \leq \frac{h}{\hat{h}} \leq \sqrt{\frac{h_{\max}}{h_{\min}}}. \quad (2.23)$$

Let  $\beta = \sqrt{\frac{h_{\max}}{h_{\min}}}$  so that

$$\beta^{-1} \leq \frac{h}{\hat{h}} \leq \beta \quad (2.24)$$

and

$$\beta^{-1}\hat{h} \leq h \leq \beta\hat{h}. \quad (2.25)$$

In addition to the bounds on the parameter estimates, the magnitude of the disturbance is known to be bounded by some maximum  $D$ :

$$|d| \leq D. \quad (2.26)$$

Finally, the error in the  $a_i$  parameters is bounded by:

$$\left| \sum_{i=1}^n (\hat{a}_i - a_i) f_i \right| \leq F. \quad (2.27)$$

### 2.2.2 Control Law for the Plant with Uncertain Parameters

The proposed control law from equation (2.10) is modified to:

$$u = \hat{h}y_r^{(n)} - k\text{sgn}(s) + \sum_{i=1}^n \hat{a}_i f_i. \quad (2.28)$$

This accounts for the fact that the parameters used in the control law were not certain, so they could not be used in the control law for the nominal system.

*Theorem:* If the proposed controller in equation (2.28) is applied to the plant that is described by equation (2.3) and estimated by equation (2.19), then  $s$  approaches zero in a finite time causing  $e$  to exponentially approach zero provided that:

$$k = |\beta - 1|\hat{h}|y_r^{(n)}| + F + D + \eta, \quad (2.29)$$

where  $\eta > 0$  and the values  $F$ ,  $D$ , and  $\beta$  are defined by the bounds on unknown parameters as discussed in section 2.2.1.

*Proof:* Consider the positive definite Lyapunov function as follows:

$$V = \frac{1}{2}hs^2. \quad (2.30)$$

The time derivative of this Lyapunov function would clearly be:

$$\dot{V} = hs\dot{s}. \quad (2.31)$$

Substituting the equation (2.9) for  $\dot{s}$  gives:

$$\dot{V} = hs\left(\frac{1}{h}\left(u - \sum_{i=1}^n a_i f_i - d\right) - y_r^{(n)}\right). \quad (2.32)$$

Use the control law from equation (2.28) for the Lyapunov analysis in the above equation:

$$\dot{V} = hs\left(\frac{1}{h}\left(\hat{h}y_r^{(n)} - k\text{sgn}(s) + \sum_{i=1}^n \hat{a}_i f_i - \sum_{i=1}^n a_i f_i - d\right) - y_r^{(n)}\right). \quad (2.33)$$

Distributing and rearranging terms leads to

$$\dot{V} = s\left(\hat{h}y_r^{(n)} - k\text{sgn}(s) + \sum_{i=1}^n (\hat{a}_i - a_i) f_i - d - hy_r^{(n)}\right), \quad (2.34)$$

which can be further reduced to

$$\dot{V} = s((\hat{h} - h)y_r^{(n)} - k\text{sgn}(s) + \sum_{i=1}^n (\hat{a}_i - a_i)f_i - d). \quad (2.35)$$

Clearly,  $s \text{sgn}(s)$  will be positive whether  $s$  is positive or negative so it can be written as  $|s|$ . Also, the bounds of the nominal parameters defined in section 2.2.1 are applied. Then, the equation is converted to an inequality with the knowledge that  $ab \leq |a||b|$ . This leads to:

$$\dot{V} \leq |s| \left| \hat{h} - h \right| |y_r^{(n)}| - k|s| + F|s| + D|s|. \quad (2.36)$$

But the worst case scenario for  $h$  is  $\beta\hat{h}$ . Also note that  $|\beta - 1| = |1 - \beta|$  so

$$\dot{V} \leq |s| (|\beta - 1| \hat{h} |y_r^{(n)}| + F + D) - k|s|. \quad (2.37)$$

Plug in equation (2.29) for  $k$  to get:

$$\dot{V} \leq |s| (|\beta - 1| \hat{h} |y_r^{(n)}| + F + D) - (|\beta - 1| \hat{h} |y_r^{(n)}| + F + D + \eta) |s|. \quad (2.38)$$

Most of the terms cancel out, leaving only:

$$\dot{V} \leq -|s|\eta. \quad (2.39)$$

Because  $\eta$  is positive,  $\dot{V}$  is negative definite. Therefore,  $V$  will vanish; hence, the combined error  $s$  and by extension the output error  $e$  will approach 0 exponentially. This concludes the proof of the theorem.

### 2.3 Control Law with a Boundary Layer

A disadvantage to the control law in equation (2.28) is that it will produce chattering behavior. As the combined error approaches zero, it will overshoot, causing it to have to correct, which will again overshoot. The error dynamics force the error to rapidly oscillate near zero, which can have detrimental effects when the real-world system, such as a motor for example, cannot handle the chattering behavior. This is addressed by modifying the control law from equation (2.28) to:

$$u = \hat{h}y_r^{(n)} + \sum_{i=1}^n \hat{a}_i f_i - k \text{sat}\left(\frac{s}{\phi_s}\right), \quad (2.40)$$

where  $\phi_s > 0$  is the boundary layer for  $s$  and  $k$  is defined by equation (2.29). The saturation function is defined as

$$\text{sat}\left(\frac{s}{\phi_s}\right) = \begin{cases} \text{sgn}\left(\frac{s}{\phi_s}\right) & \text{if } |s| \geq \phi_s \\ \frac{s}{\phi_s} & \text{if } |s| \leq \phi_s \end{cases}. \quad (2.41)$$

*Theorem:* If the proposed controller in equation (2.40) with  $k$  from equation (2.29) is applied to the plant that is described by equation (2.3) and estimated

by equation (2.19), then  $s$  enters the boundary layer and decreases until:

$$|s|_{ss} \leq \frac{A\phi_s}{A + \eta} < \phi_s, \quad (2.42)$$

where

$$A = (\beta - 1)\hat{h}|y_r^{(n)}| + F + D \quad (2.43)$$

and  $|s|_{ss}$  is the steady state  $|s|$ .

*Proof:* Outside the boundary layer,  $\text{sat}(\frac{s}{\phi_s}) = \text{sgn}(\frac{s}{\phi_s}) = \text{sgn}(s)$  so equation (2.40) is equivalent to equation (2.28) outside the boundary layer. Hence, by the previous theorem, the control law still converges to the boundary layer the same way. Inside the boundary layer,  $\text{sat}(\frac{s}{\phi_s}) = \frac{s}{\phi_s}$  so within the boundary layer, equation (2.40) is equivalent to

$$u = \hat{h}y_r^{(n)} + \sum_{i=1}^n \hat{a}_i f_i - k \frac{s}{\phi_s}. \quad (2.44)$$

Consider the following Lyapunov function

$$V = \frac{1}{2}hs^2 \quad (2.45)$$

with the time derivative of

$$\dot{V} = hss. \quad (2.46)$$

Using equation (2.9) for  $\dot{s}$ , this becomes

$$\dot{V} = hs\left(\frac{1}{h}\left(u - \sum_{i=1}^n a_i f_i - d\right) - y_r^{(n)}\right). \quad (2.47)$$

Distributing the  $h$  term and plugging in the equation (2.44) for the controller with the boundary layer, we get

$$\dot{V} = s(\hat{h}y_r^{(n)} + \sum_{i=1}^n \hat{a}_i f_i - k\frac{s}{\phi_s} - \sum_{i=1}^n a_i f_i - d - hy_r^{(n)}), \quad (2.48)$$

and

$$\dot{V} = s((\hat{h} - h)y_r^{(n)} + \sum_{i=1}^n (\hat{a}_i - a_i)f_i - k\frac{s}{\phi_s} - d). \quad (2.49)$$

Note that for the worst case,  $\hat{h} - h = \hat{h} - \beta\hat{h} = (1 - \beta)\hat{h}$ . Applying this as well as the bounds on the parameters and disturbance as defined in section 2.2.1, we get

$$\dot{V} \leq |s||1 - \beta|\hat{h}|y_r^{(n)}| + F|s| + D|s| - k\frac{s^2}{\phi_s}. \quad (2.50)$$

Because  $\beta > 1$ , we have  $|1 - \beta| = \beta - 1$  and choosing  $A$  according to equation (2.43), then

$$\dot{V} \leq A|s| - k\frac{s^2}{\phi_s}. \quad (2.51)$$

Substituting for  $k$  from equation (2.29) and simplifying, we get:

$$\dot{V} \leq A|s| - (A + \eta)\frac{s^2}{\phi_s}. \quad (2.52)$$

Clearly,  $\dot{V} \leq 0$  (and by extension  $s$  is decreasing) for all values of  $s$  if:

$$A|s| - (A + \eta) \frac{s^2}{\phi_s} < 0, \quad (2.53)$$

which leads to

$$A - (A + \eta) \frac{|s|}{\phi_s} < 0, \quad (2.54)$$

$$A < (A + \eta) \frac{|s|}{\phi_s}, \quad (2.55)$$

and finally,

$$\frac{A\phi_s}{A + \eta} < |s|. \quad (2.56)$$

Note that while  $|s| > \frac{A\phi_s}{A + \eta}$ ,  $\dot{V} < 0$  so  $V$  (and by extension  $s$ ) decreases. Thus,  $|s|$  will decrease until it becomes equal to  $\frac{A\phi_s}{A + \eta}$ , at which point  $\dot{V} = 0$  so  $|s|$  will stay at the steady state value  $|s|_{ss} = \frac{A\phi_s}{A + \eta}$  which is within the boundary layer since  $\frac{A}{A + \eta} < 1$ . Also note that this steady state error could theoretically be decreased by using a smaller  $\phi_s$  or a higher  $\eta$ .

## 2.4 Simulation

To demonstrate the results of this chapter, the control law was applied to a system in a simulation. The implementation of the simulation is shown below in Figure 2.1 with the relevant equations from this chapter.

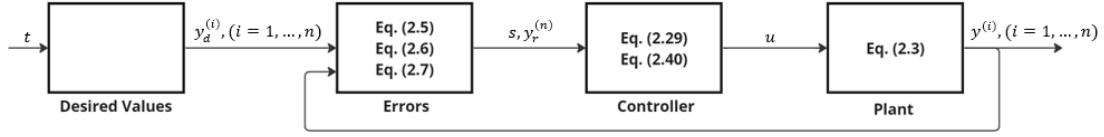


**Figure 2.1:** Block diagram of control law implementation.

### 2.4.1 Definition of Values

The system chosen for simulation was the stable fourth-order system:

$$(p + \lambda_f)^4 y = \frac{1}{h} u, \quad (2.57)$$

where  $p$  is the Laplace operator and both  $\lambda_f$  and  $h$  are greater than zero. This expands to the time-domain equation:

$$y^{(4)} + 4\lambda_f y^{(3)} + 6\lambda_f^2 y^{(2)} + 4\lambda_f^3 \dot{y} + \lambda_f^4 y = \frac{1}{h} u. \quad (2.58)$$

The functions and parameters of this system corresponding to equation (2.3) are listed in the table below, along with the estimated parameters. The parameter  $\lambda_f$  was chosen as  $\lambda_f = 0.25$  and the final parameter  $h$  was estimated as  $h_{\max} = 1.4$  and  $h_{\min} = 0.9$ . The desired trajectory for  $y$  was

$$y_d = 2 \cos(t) - \sin(t/3) + \frac{1}{12}. \quad (2.59)$$

The actual disturbance was chosen as  $d = 20$  for the time period  $7 < t < 9$  and  $d = 0$  elsewhere. In the process of tuning the  $\phi_s$  values, it was discovered that

**Table 2.1:** System functions with actual and estimated parameters.

$i$	1	2	3	4
$f$	$y$	$\dot{y}$	$y^{(2)}$	$y^{(3)}$
$a$	$\lambda_f^4$	$4\lambda_f^3$	$6\lambda_f^2$	$4\lambda_f$
$\hat{a}$	$1.5\lambda_f^4$	$3\lambda_f^3$	$8\lambda_f^2$	$2\lambda_f$

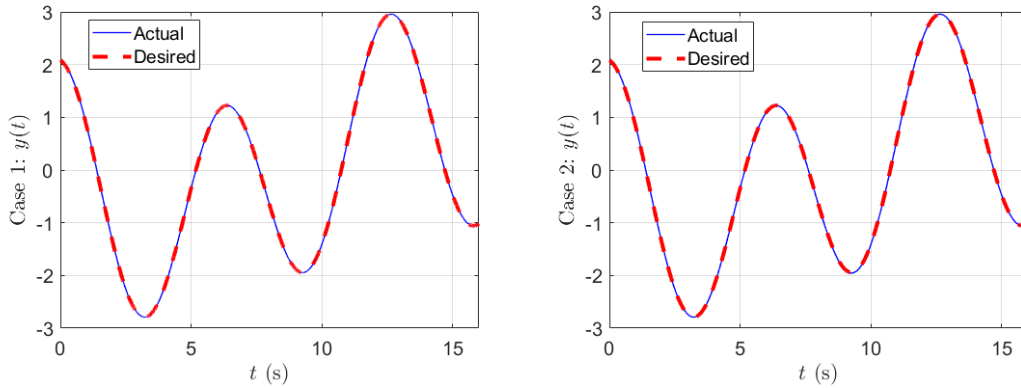
**Table 2.2:** Initial conditions and control parameters.

	$y(0)$	$\dot{y}(0)$	$\ddot{y}(0)$	$y^{(3)}(0)$	$\eta$	$\lambda$	$D$	$\phi_s$
Case 1	$\frac{25}{12}$	$-\frac{1}{3}$	-1.74	$\frac{1}{27}$	0.05	3	21	0.05
Case 2	$\frac{25}{12}$	$-\frac{1}{3}$	-1.74	$\frac{1}{27}$	0.05	3	21	0.3

a boundary layer greater than approximately 0.25 was necessary to completely eliminate chatter, although a smaller boundary layer did still attenuate the chatter significantly. Two separate cases with a smaller and a larger boundary value are compared in the results section. In both cases, the actual plant state was initialized to have zero error for  $e$ ,  $\dot{e}$ , and  $e^{(3)}$  but with an error in the acceleration of  $\ddot{e} = 0.26$ . The initial conditions as well as the gain values are listed in table 2.2.

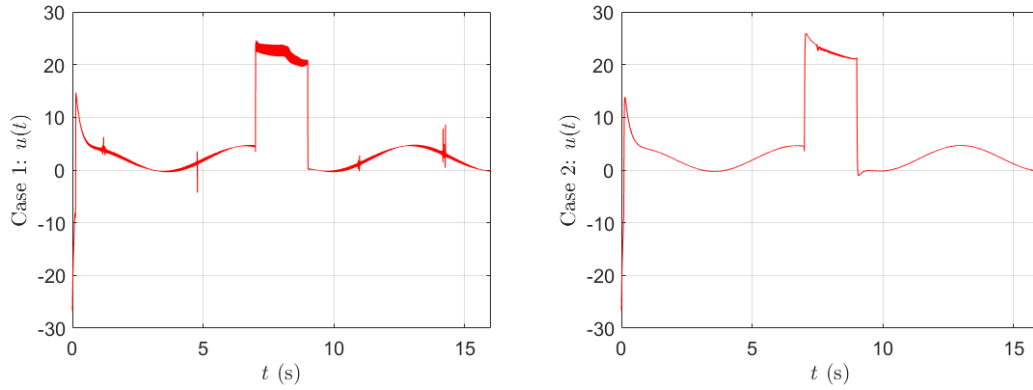
## 2.4.2 Simulation Results

Figure 2.2 shows that the controller does indeed provide tracking control for both the smaller and the larger boundary value. It can be seen in Figure 2.3



**Figure 2.2:** Actual and desired system state vs time.

that the control input does not suffer from chattering in the second case as would commonly affect an SMC using  $\text{sgn}(s)$  instead of our  $\text{sat}(s)$ . However, the first case, with the smaller boundary value, does still have chatter at several points, particularly when the disturbance is present. Figure 2.4 demonstrates that  $s$  does converge to the boundary layer, as expected for both cases. Even when the disturbance is added,  $s$  stays within the boundary layer. Because of the steep convergence of  $s$ , Figure 2.5 shows a more detailed plot of the first 0.5 seconds for both cases. When outside the boundary layer, both cases converge at the same rate, which would be expected as the only difference is the size of the boundary layer. Case 2 does reach the larger boundary layer sooner, which slows it down earlier than case 1. The result is slightly slower convergence within the boundary



**Figure 2.3:** Control input vs time.

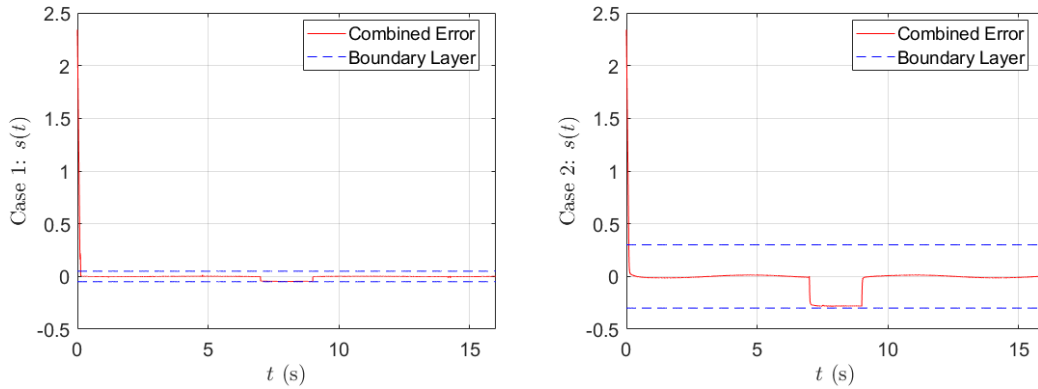


**Figure 2.4:** Combined error vs time (the whole simulation duration).

layer. Finally, the state error, plotted in Figure 2.6, does converge to a steady-state value near zero quite quickly for both cases. The disturbance does affect the second case error significantly more than the first because  $s$  has not converged as much for the second case when the disturbance is added. Theoretically, both the combined error and the state error should converge to smaller steady-state values for the first case, according to the theorem in section 2.3. This was not the case in the simulation, however. As Table 2.3 shows, we did have a smaller

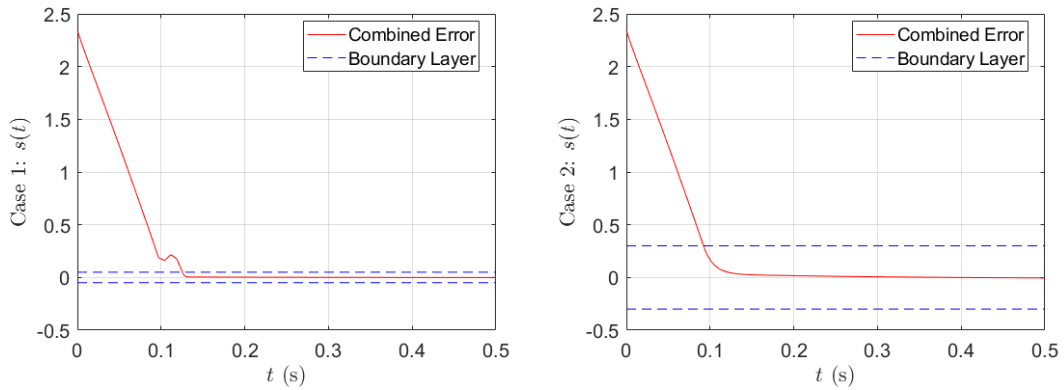


**Figure 2.5:** Combined error vs time (the first 0.5 seconds).

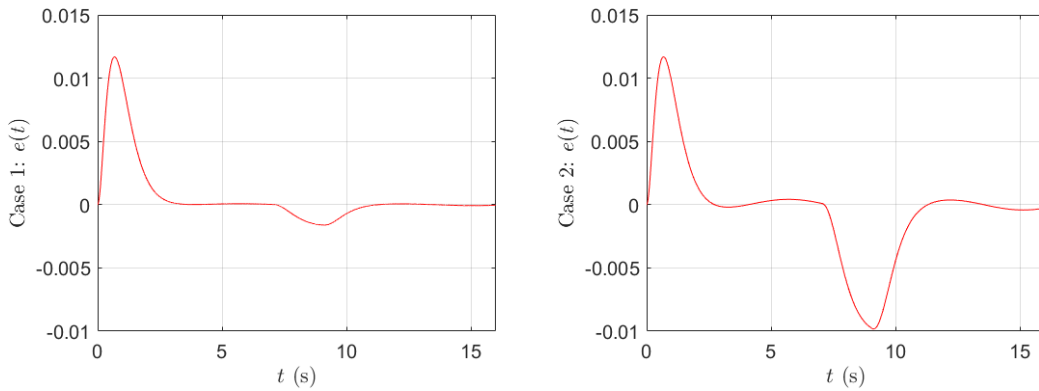


**Figure 2.6:** State error vs time.

steady-state  $e$  but had a roughly similar steady-state  $s$ . This is likely because of the chattering, which prevented it from converging to the theoretical steady-state value due to the simulation using a discrete time step. The smaller boundary layer has the theoretical advantage of a smaller steady-state error for  $s$  and  $e$  and slightly quicker convergence but in practice has the disadvantage of not completely attenuating chatter. This motivates the search for an adaptive boundary layer

**Table 2.3:** Combined and state errors.

	$s_{ss}$	$e_{ss}$	$e_{\min}$	$e_{\max}$
Case 1	$1.50 * 10^{-2}$	$0.74 * 10^{-4}$	-0.0016	0.0117
Case 2	$1.38 * 10^{-2}$	$4.20 * 10^{-4}$	-0.0098	0.0117

that shrinks to reduce the steady-state error, but grows when chatter is present.

This adaptive boundary layer will be derived in chapter 3.

## Chapter 3. Adaptive Boundary Layer Sliding Mode Controller for a Plant with Uncertain Parameters

In this section, a control method is derived for a plant in which uncertain parameters are bounded by known values and a sliding mode control method with a varying boundary layer is used. The goal of using a varying boundary layer is to make the control law more robust to large disturbances. If large disturbances are dealt with by increasing  $\eta$  and thus  $k$  as well, this increases  $\dot{s}$  which can cause chattering if too large. A boundary layer that increases when large disturbances to the system are present can fix this problem. In section 3.1, the problem statement and control law from the chapter 2 are restated more concisely. In section 3.2, a lemma for the error behavior required for convergence with a varying boundary layer is derived. In section 3.3, the control law from chapter 2 is modified and shown by Lyapunov analysis to produce convergence.

## 3.1 Problem Statement and Control Law

### 3.1.1 Plant Model

The plant to be controlled is defined by the equation:

$$y^{(n)} + \sum_{i=1}^n \alpha_i f_i = bu + \delta, \quad (3.1)$$

where  $y$  is the state of the plant,  $u$  is the control input,  $\delta$  is the disturbance to the plant, and  $f_i$  are known, nonlinear functions. The parameters  $\alpha_i$  and  $b$  are the true plant parameters in the above equation, but these are not known, so they are estimated with the variables  $\hat{\alpha}_i$  and  $\hat{b}$ . The nominal plant model is then:

$$y^{(n)} + \sum_{i=1}^n \hat{\alpha}_i f_i = \hat{b}u + \delta. \quad (3.2)$$

Like in chapter 2, the plant model can also be rewritten using the following variables substituted when appropriate:

$$h = 1/b, a_i = \frac{\alpha_i}{b}, d = -\delta/b. \quad (3.3)$$

The true and nominal plant models then become:

$$hy^{(n)} + \sum_{i=1}^n a_i f_i + d = u \quad (3.4)$$

and

$$\hat{h}y^{(n)} + \sum_{i=1}^n \hat{a}_i f_i + d = u. \quad (3.5)$$

The state error for the system is defined as

$$e = y - y_d, \quad (3.6)$$

where  $y_d$  is the desired output. The state error dynamics are then

$$e^{(n-1)} = y^{(n-1)} - y_d^{(n-1)}. \quad (3.7)$$

This is used to define the combined error as

$$s = e^{(n-1)} + \sum_{i=0}^{n-2} \binom{n-1}{i} \lambda^{n-i-1} e^{(i)}. \quad (3.8)$$

This guarantees that if the combined error  $s$  vanishes, then the state error  $e$  exponentially approaches 0 for any positive  $\lambda$ . The reference value  $y_r^{(n)}$  is again defined as:

$$y_r^{(n)} = y_d^{(n)} - \sum_{i=0}^{n-2} \binom{n-1}{i} \lambda^{n-i-1} e^{(i+1)}. \quad (3.9)$$

Taking the derivative of the combined error equation (3.8) and substituting the above equation into the result gives the combined error dynamics as:

$$\dot{s} = y^{(n)} - y_r^{(n)}. \quad (3.10)$$

### 3.1.2 Bounds on Uncertain Parameters

In the nominal system, the estimates  $\hat{a}_i$  and  $\hat{h}$  are bounded by known values. The error in the  $a_i$  parameters is bounded by:

$$\left| \sum_{i=1}^n (\hat{a}_i - a_i) f_i \right| \leq F. \quad (3.11)$$

The parameter  $h$  is again bounded as

$$0 < h_{\min} \leq h \leq h_{\max}. \quad (3.12)$$

The same analysis as done in section 2.2.1 leads to:

$$\beta^{-1} \hat{h} \leq h \leq \beta \hat{h}, \quad (3.13)$$

where  $\beta$  is defined as  $\beta = \sqrt{\frac{h_{\max}}{h_{\min}}} > 0$ . In addition to the bounds on the parameter estimates, the magnitude of the disturbance is known to be bounded by some maximum  $D$ :

$$|d| \leq D. \quad (3.14)$$

### 3.1.3 Control Law

The control law to control the above system with a constant boundary layer was found in chapter 2 to be:

$$u = \hat{h}y_r^{(n)} + \sum_{i=1}^n \hat{a}_i f_i - k \text{sat}\left(\frac{s}{\phi_s}\right), \quad (3.15)$$

where the gain  $k$  was

$$k = |\beta - 1| \hat{h} |y_r^{(n)}| + F + D + \eta \quad (3.16)$$

with  $\eta$  as a positive constant.

### 3.2 Required Error Behavior for Varying Boundary Layer

*Lemma:* Consider the system described in section 3.1 modified to use a varying boundary layer. For  $s$  to approach the boundary layer when outside,  $s\dot{s} \leq (\dot{\phi}_s - \frac{\eta}{h})|s|$  proves this convergence.

*Proof:* Suppose  $s > \phi_s > 0$ . Then  $s$  clearly approaches  $\phi_s$  if and only if:

$$\frac{d}{dt}(s - \phi_s) \leq -\frac{\eta}{h}, \quad (3.17)$$

where  $\eta > 0$ . Applying the derivative gives the equation:

$$\dot{s} - \dot{\phi}_s \leq -\frac{\eta}{h}, \quad (3.18)$$

which leads to:

$$\dot{s} \leq (\dot{\phi}_s - \frac{\eta}{h}). \quad (3.19)$$

But  $s > 0$ , so  $s = |s|$  and:

$$s\dot{s} \leq (\dot{\phi}_s - \frac{\eta}{h})|s|. \quad (3.20)$$

Alternatively, suppose  $s < -\phi_s < 0$ . Then clearly  $s$  approaches  $-\phi_s$  if and only if:

$$\frac{d}{dt}(s - (-\phi_s)) \geq \frac{\eta}{h}, \quad (3.21)$$

where  $\eta > 0$ . Applying the derivative gives the equation:

$$\dot{s} + \dot{\phi}_s \geq \frac{\eta}{h}, \quad (3.22)$$

which leads to:

$$\dot{s} \geq (\frac{\eta}{h} - \dot{\phi}_s). \quad (3.23)$$

But  $s < 0$  so  $s = -|s|$  and multiplying by  $s$  flips the inequality:

$$s\dot{s} \leq (\dot{\phi}_s - \frac{\eta}{h})|s|. \quad (3.24)$$

Hence,  $s$  converges to the boundary layer if  $s\dot{s} \leq (\dot{\phi}_s - \frac{\eta}{h})|s|$ .

### 3.3 Control Law for Varying Boundary Layer

To control the plant using a varying boundary layer, the following control law is proposed:

$$u = \hat{h}y_r^{(n)} + \sum_{i=1}^n \hat{a}_i f_i - \bar{k} \text{sat}\left(\frac{s}{\phi_s}\right), \quad (3.25)$$

where the modified gain is calculated as:

$$\bar{k} = \begin{cases} (k - \beta \hat{h} \dot{\phi}_s) & \text{if } \dot{\phi}_s \leq 0 \\ (k - \beta^{-1} \hat{h} \dot{\phi}_s) & \text{if } \dot{\phi}_s \geq 0 \end{cases} \quad (3.26)$$

using the original gain from (3.16).

#### 3.3.1 Outside the Boundary Layer

*Theorem:* If the SMC control law from equations (3.25) and (3.26) is applied to the plant described by equation (3.4) and estimated by equation (3.5), then  $s$  approaches the boundary layer in a finite time.

*Proof:* As the lemma in the previous section demonstrated, the goal is to show that  $s\dot{s} \leq (\dot{\phi}_s - \frac{\eta}{h})|s|$  when outside the boundary layer. From equation (3.10) with  $y^{(n)}$  from equation (3.4), the error dynamics becomes:

$$\dot{s} = \frac{1}{h} \left( u - \sum_{i=1}^n a_i f_i - d \right) - y_r^{(n)}. \quad (3.27)$$

Plugging in the value for  $u$  from equation (3.25) gives

$$\dot{s} = \frac{1}{h}(\hat{h}y_r^{(n)} + \sum_{i=1}^n \hat{a}_i f_i - \bar{k}\text{sat}(\frac{s}{\phi_s}) - \sum_{i=1}^n a_i f_i - d) - y_r^{(n)}. \quad (3.28)$$

Algebraically manipulating the equation allows us to write this as

$$\dot{s} = \frac{1}{h}(\hat{h} - h)y_r^{(n)} + \frac{1}{h}(\sum_{i=1}^n (\hat{a}_i - a_i)f_i - \bar{k}\text{sat}(\frac{s}{\phi_s}) - d). \quad (3.29)$$

Then, to get an equation of the correct form to be compared to equation (3.24) from the lemma, the above equation is multiplied by  $s$  and maximized to get an inequality:

$$s\dot{s} \leq |s|\frac{1}{h}|\hat{h} - h||y_r^{(n)}| + |s|\frac{1}{h}\left|\sum_{i=1}^n (\hat{a}_i - a_i)f_i\right| - s\frac{1}{h}\bar{k}\text{sat}(\frac{s}{\phi_s}) + |s|\frac{1}{h}|d|. \quad (3.30)$$

Because this is outside the boundary layer,  $\text{sat}(\frac{s}{\phi_s}) = \text{sgn}(\frac{s}{\phi_s}) = \text{sgn}(s)$ . This and the bounds from (3.11), (3.14), and (3.13) are used to reduce the inequality to

$$s\dot{s} \leq |s|\frac{\hat{h}}{h}|\beta - 1||y_r^{(n)}| + |s|\frac{1}{h}F - |s|\frac{1}{h}\bar{k} + |s|\frac{1}{h}D. \quad (3.31)$$

This can now be set equal to the equation (3.24) from the lemma:

$$(\dot{\phi}_s - \frac{\eta}{h})|s| = |s|\frac{\hat{h}}{h}|\beta - 1||y_r^{(n)}| + |s|\frac{1}{h}F - |s|\frac{1}{h}\bar{k} + |s|\frac{1}{h}D. \quad (3.32)$$

Dividing everything by  $|s|$  and isolating  $\bar{k}$  leads to

$$\bar{k} = \hat{h}|\beta - 1||y_r^{(n)}| + F + D + \eta - h\dot{\phi}_s. \quad (3.33)$$

Plugging in the equation (3.16) for  $k$  then results in

$$\bar{k} = k - h\dot{\phi}_s. \quad (3.34)$$

Note that the value of  $h$  is unknown. However, we know the lower bound and the upper bound of  $h$  using equation (3.13). We use the bounds to maximize  $\bar{k}$  all the time for faster convergence to the sliding surface. To that end, if  $\dot{\phi}_s > 0$ , we use the lower bound of  $h_{\min} = \beta^{-1}\hat{h}$  instead of  $h$ , and, if  $\dot{\phi}_s < 0$ , we use the upper bound of  $h_{\max} = \beta\hat{h}$  instead of  $h$ . This can be written as

$$\bar{k} = \begin{cases} (k - \beta\hat{h}\dot{\phi}_s) & \text{if } \dot{\phi}_s \leq 0 \\ (k - \beta^{-1}\hat{h}\dot{\phi}_s) & \text{if } \dot{\phi}_s \geq 0 \end{cases}. \quad (3.35)$$

This concludes the proof of the theorem.

### 3.3.2 Deriving the Boundary Layer Adaptation Law

Note that when  $s$  is within the boundary layer, it decays exponentially. This rate of decay should be greater than the rate of decay for  $e$ .

*Theorem:* The following boundary layer adaptation law for  $\phi_s$  defined by:

$$\dot{\phi}_s = \begin{cases} \frac{k_d}{\beta h} - \lambda \phi_s & \text{if } \frac{k_d}{\beta h} \leq \lambda \phi_s, \\ \frac{\beta k_d}{h} - \lambda \beta^2 \phi_s & \text{if } \frac{k_d}{\beta h} \geq \lambda \phi_s \end{cases}, \quad (3.36)$$

where  $k_d = k(y_d)$  satisfies the requirement for a greater rate of decay of  $s$  than the rate of decay for  $e$ .

*Proof:* Inside the boundary layer,  $\text{sat}(\frac{s}{\phi_s}) = \frac{s}{\phi_s}$  so equation (3.29) becomes

$$\dot{s} = \frac{1}{h}(\hat{h} - h)y_r^{(n)} + \frac{1}{h}\left(\sum_{i=1}^n (\hat{a}_i - a_i)f_i - \bar{k}\frac{s}{\phi_s} - d\right). \quad (3.37)$$

Because this is inside the boundary layer, the errors are considered small, and it is reasonable to assume that  $y^{(n)} \approx y_d^{(n)}$ . Also, all the output errors  $e^i$  are near zero, so  $y_r^{(n)} \approx y_d^{(n)}$ . Then, assuming the disturbance is close to zero,  $\dot{s}$  becomes

$$\dot{s} \approx \frac{1}{h}(\hat{h} - h)y_d^{(n)} + \frac{1}{h}\left(\sum_{i=1}^n \Delta a_i f_i - \bar{k}\frac{s}{\phi_s}\right) \quad (3.38)$$

$$\dot{s} = H(y_d) + O(\epsilon) - \frac{1}{h}\bar{k}(y_d)\frac{s}{\phi_s}. \quad (3.39)$$

In the above equation,  $H(y_d) + O(\epsilon)$  is the combined effect of all the uncertainties in the system. This error is bounded, since both the true parameters and the estimates of those parameters are bounded. The equation is a stable first order filter with  $H(y_d) + O(\epsilon)$  as the input and  $s$  as the output. Because the input is bounded, the output must be bounded as well. The decay of  $s$  is then determined

based on the coefficient on the  $s$  term. The rate of decay of  $s$  within the boundary layer is:

$$\frac{1}{h} \frac{\bar{k}(y_d)}{\phi_s} = \lambda_s. \quad (3.40)$$

To make  $\lambda_s$  (the rate of decay of  $s$ ) greater than  $\lambda$  (the rate of decay of  $e$ ),

$$\lambda_s = \frac{h_{\max}}{h} \lambda. \quad (3.41)$$

Substituting  $\lambda_s$  from equation (3.40) in the above equation and noting that  $h_{\max} = \beta \hat{h}$ , we get:

$$\frac{\bar{k}(y_d)}{\phi_s} = \lambda \beta \hat{h}. \quad (3.42)$$

Solving this for the gain,

$$\bar{k}(y_d) = \lambda \beta \phi_s \hat{h}, \quad (3.43)$$

and then plug this into equation (3.35) for  $\dot{\phi}_s \leq 0$  for the first case to get

$$\lambda \beta \phi_s \hat{h} = k(y_d) - \beta \hat{h} \dot{\phi}_s \quad \text{for } \dot{\phi}_s \leq 0 \quad (3.44)$$

and for  $\dot{\phi}_s \geq 0$  for the second case to get

$$\lambda \beta \phi_s \hat{h} = k(y_d) - \beta^{-1} \hat{h} \dot{\phi}_s \quad \text{for } \dot{\phi}_s \geq 0. \quad (3.45)$$

Solving (3.44) and (3.45) for  $\dot{\phi}_s$  results in

$$\dot{\phi}_s = \begin{cases} \frac{k_d}{\beta \hat{h}} - \lambda \phi_s & \text{if } \frac{k_d}{\beta \hat{h}} \leq \lambda \phi_s \\ \frac{\beta k_d}{\hat{h}} - \lambda \beta^2 \phi_s & \text{if } \frac{k_d}{\beta \hat{h}} \geq \lambda \phi_s \end{cases}, \quad (3.46)$$

where  $k_d = k(y_d)$ . This, then, will be the control law for the boundary layer.

### 3.3.3 Steady-State Boundary Layer Thickness

*Lemma:* Using the control law for the boundary layer as defined in equation (3.46) will cause the boundary layer to converge to the steady-state value

$$\{\phi_s\}_{ss} = \frac{k}{\beta \hat{h} \lambda}.$$

*Proof:* If  $\frac{k_d}{\beta \hat{h}} \leq \lambda \phi_s$ , then using equation (3.46) we can see that  $\dot{\phi}_s = \frac{k_d}{\beta \hat{h}} - \lambda \phi_s$ . When  $\frac{k_d}{\beta \hat{h}} < \lambda \phi_s$ , then  $\dot{\phi}_s < 0$ . Therefore,  $\phi_s$  will decrease until  $\dot{\phi}_s = 0$ . Setting  $\dot{\phi}_s = 0$ , we get

$$\frac{k_d}{\beta \hat{h}} - \lambda \phi_s = 0. \quad (3.47)$$

Solving for  $\phi_s$ , we get

$$\phi_s = \frac{k_d}{\beta \hat{h} \lambda}. \quad (3.48)$$

Similarly, when  $\frac{k_d}{\beta \hat{h}} \geq \lambda \phi_s$ , then using equation (3.46) we can see that  $\dot{\phi}_s = \frac{\beta k_d}{\hat{h}} - \lambda \beta^2 \phi_s$ . When  $\frac{k_d}{\beta \hat{h}} > \lambda \phi_s$ , then  $\frac{\beta k_d}{\hat{h}} > \lambda \beta^2 \phi_s$  so  $\dot{\phi}_s > 0$ . Therefore,  $\phi_s$  will increase until  $\dot{\phi}_s = 0$ . Setting  $\dot{\phi}_s = 0$ , we get

$$\frac{\beta k_d}{\hat{h}} - \lambda \beta^2 \phi_s = 0. \quad (3.49)$$

Solving for  $\phi_s$ , we get

$$\phi_s = \frac{k_d}{\beta \hat{h} \lambda}. \quad (3.50)$$

Thus, according to equations (3.48) and (3.50), the boundary layer does reach a steady state value where  $\dot{\phi}_s = 0$  when

$$\{\phi_s\}_{ss} = \frac{k_d}{\beta \hat{h} \lambda}. \quad (3.51)$$

Note that increasing  $\lambda$  decreases the steady-state boundary layer thickness.

### 3.3.4 Steady-state $s$ inside the Boundary Layer

*Theorem:* If the SMC control law from equations (3.25), (3.26), and (3.36) is applied to the plant described by equation (3.4) and estimated by equation (3.5), then, once it initially reaches the boundary layer,  $s$  will stay within the boundary layer and converge to a steady-state value  $|s|_{ss} \leq \frac{A}{\beta \hat{h} \lambda}$  where  $A$  is defined as  $A = \hat{h}(\beta - 1) \left| y_r^{(n)} \right| + F + D$ .

*Proof:* Consider the positive definite Lyapunov function

$$V = \frac{1}{2} h s^2 \quad (3.52)$$

with the time derivative of

$$\dot{V} = h s \dot{s}. \quad (3.53)$$

Plugging in equation (3.10) for  $\dot{s}$  with equation (3.4) for  $y^{(n)}$  gives us

$$\dot{V} = hs\left(\frac{1}{h}\left(u - \sum_{i=1}^n a_i f_i - d\right) - y_r^{(n)}\right). \quad (3.54)$$

Using our control input from equation (3.25),

$$\dot{V} = hs\left(\frac{1}{h}\left(\hat{h}y_r^{(n)} + \sum_{i=1}^n \hat{a}_i f_i - \bar{k}\text{sat}\left(\frac{s}{\phi_s}\right) - \sum_{i=1}^n a_i f_i - d\right) - y_r^{(n)}\right), \quad (3.55)$$

which leads to

$$\dot{V} = s\left((\hat{h} - h)y_r^{(n)} + \sum_{i=1}^n (\hat{a}_i - a_i)f_i - \bar{k}\text{sat}\left(\frac{s}{\phi_s}\right) - d\right). \quad (3.56)$$

Inside the boundary layer,  $\text{sat}\left(\frac{s}{\phi_s}\right) = \frac{s}{\phi_s}$  so this becomes

$$\dot{V} = s\left((\hat{h} - h)y_r^{(n)} + \sum_{i=1}^n (\hat{a}_i - a_i)f_i - \bar{k}\frac{s}{\phi_s} - d\right). \quad (3.57)$$

Maximizing the right-hand side of the equation produces the inequality as follows:

$$\dot{V} \leq |s|\left|\hat{h} - h\right|\left|y_r^{(n)}\right| + |s|\left|\sum_{i=1}^n (\hat{a}_i - a_i)f_i\right| - \bar{k}\frac{s^2}{\phi_s} + |s||d|. \quad (3.58)$$

Using the bounds from section 3.1.2, we arrive at

$$\dot{V} \leq |s|\hat{h}(\beta - 1)\left|y_r^{(n)}\right| + |s|F - \bar{k}\frac{s^2}{\phi_s} + |s|D. \quad (3.59)$$

Then choose  $A = \hat{h}(\beta - 1) \left| y_r^{(n)} \right| + F + D$  so that

$$\dot{V} \leq |s|A - \bar{k} \frac{s^2}{\phi_s}. \quad (3.60)$$

So the Lyapunov derivative is less than zero if

$$|s|A - \bar{k} \frac{s^2}{\phi_s} \leq 0. \quad (3.61)$$

This implies that

$$A\phi_s \leq \bar{k}|s|. \quad (3.62)$$

*Case 1: Decreasing Boundary Layer*

If the boundary layer is decreasing, then  $\dot{\phi}_s < 0$  so the gain is  $\bar{k} = k - \beta \hat{h} \dot{\phi}_s > 0$ . Thus, equation (3.62) becomes

$$\frac{A\phi_s}{\bar{k}} \leq |s|. \quad (3.63)$$

Plugging in  $\bar{k}$  gives us

$$\frac{A\phi_s}{k - \beta \hat{h} \dot{\phi}_s} \leq |s|. \quad (3.64)$$

Then substituting for  $\dot{\phi}_s$  for case 1 results in

$$\frac{A\phi_s}{k - \beta \hat{h} \left( \frac{\beta-1}{\hat{h}} k - \lambda \phi_s \right)} \leq |s|. \quad (3.65)$$

Simplifying this, we get

$$\frac{A}{\beta \hat{h} \lambda} \leq |s|. \quad (3.66)$$

*Case 2: Increasing Boundary Layer*

If the boundary layer is increasing, then  $\dot{\phi}_s > 0$  so the gain is  $\bar{k} = k - \beta^{-1} \hat{h} \dot{\phi}_s$ . Thus, equation (3.62) becomes

$$A \phi_s \leq (k - \beta^{-1} \hat{h} \dot{\phi}_s) |s|. \quad (3.67)$$

Then substituting for  $\dot{\phi}_s$  for case 2, we get

$$A \phi_s \leq (k - \beta^{-1} \hat{h} (\frac{\beta}{\hat{h}} k - \lambda \beta^2 \phi_s)) |s|. \quad (3.68)$$

Simplifying this, we arrive at

$$\frac{A}{\beta \hat{h} \lambda} \leq |s|. \quad (3.69)$$

Therefore, whether  $\phi_s$  is increasing or decreasing,  $\dot{V}$  is negative definite for any  $|s| \geq \frac{A}{\beta \hat{h} \lambda}$ . Hence,  $|s|$  will converge to some steady-state value  $|s|_{ss} = \frac{A}{\beta \hat{h} \lambda}$ . Note that this steady-state error can be reduced by using a larger  $\lambda$ . This concludes the proof of the theorem.

*Lemma:* Using the control law from equations (3.25), (3.26), and (3.36), the combined error  $s$  will stay within the boundary layer once it has converged to its steady-state value.

*Proof:* According to the previous theorem, the combined error converges to the steady-state value  $|s|_{ss} = \frac{A}{\beta \hat{h} \lambda}$ . According to the lemma in section 3.3.3, the

boundary layer converges to the steady-state value  $\{\phi_s\}_{ss} = \frac{k}{\beta \hat{h} \lambda}$ . From equation (3.16),  $k = |\beta - 1| \hat{h} |y_r^{(n)}| + F + D + \eta = A + \eta$ . Thus, the steady-state value for  $\phi_s$  can be written as

$$\{\phi_s\}_{ss} = |s|_{ss} + \frac{\eta}{\beta \hat{h} \lambda}. \quad (3.70)$$

Because  $\eta$  is greater than zero, the steady-state value for  $\phi_s$  is greater than the steady-state value for  $s$ . In other words, the combined error converges to a steady-state value within the boundary layer.

### 3.4 Simulation

To demonstrate the results of this chapter, the control law was applied to a system in a simulation. The implementation of the simulation is shown below in Figure 2.1 with the relevant equations from this chapter.

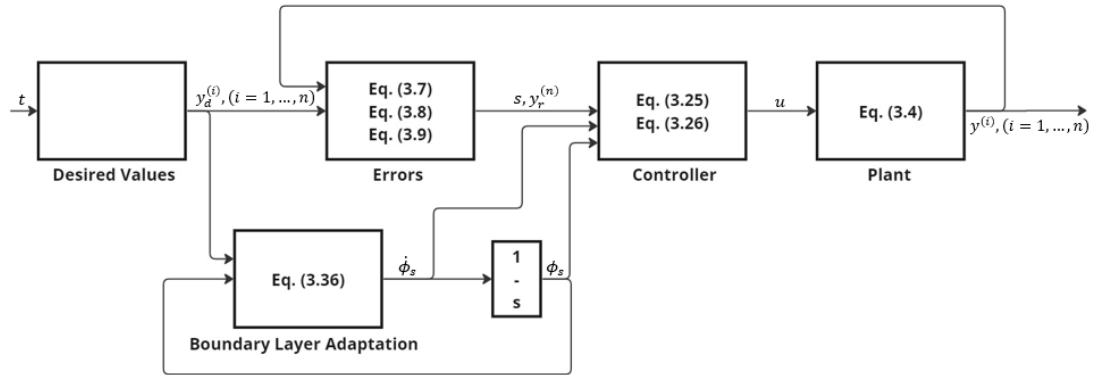


**Figure 3.1:** Block diagram of control law implementation.

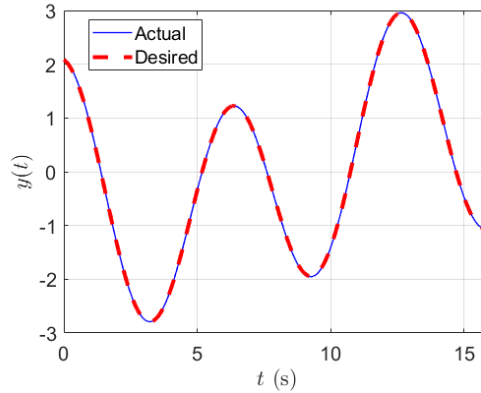
The same system and desired trajectory from section 2.4.1 were used with the same gain values and parameters. Additionally, the same set of initial condi-

tions were used. The only modification to note is that the varying boundary value was initialized at  $\phi_s(0) = 1$  instead of the constant 0.05 or 0.3 in the previous chapter.

**Table 3.1:** Initial conditions and control parameters.

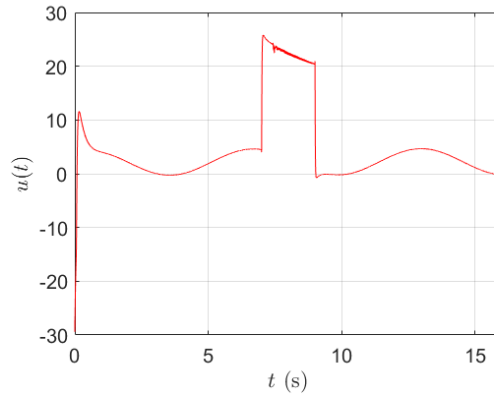
$y(0)$	$\dot{y}(0)$	$\ddot{y}(0)$	$y^{(3)}(0)$	$\eta$	$\lambda$	$D$	$\phi_s(0)$
$\frac{25}{12}$	$-\frac{1}{3}$	-1.74	$\frac{1}{27}$	0.05	3	21	1

Figure 3.2 shows that the controller does indeed provide tracking control. It can be seen in Figure 3.3 that the control input once again does not suffer



**Figure 3.2:** Actual and desired system state vs time.

from chattering due to our use of  $\text{sat}(\frac{s}{\phi_s})$  instead of  $\text{sgn}(s)$ . As mentioned in the previous chapter, a boundary layer greater than approximately 0.25 was necessary to completely eliminate chatter, although a smaller boundary layer did still dampen the chatter significantly. Even though we initialized our boundary layer at  $\phi_s(0) = 1$ , our adaptive law for the boundary layer decreased it to a value



**Figure 3.3:** Control input vs time.

that reduced the steady-state error but still eliminated chatter. Figure 3.4 plots

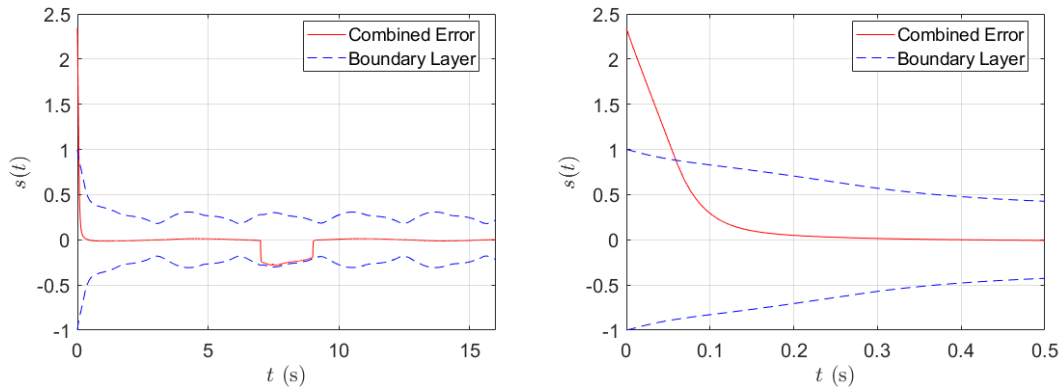


**Figure 3.4:** Combined error vs time (left: entire duration, right: first 0.5 seconds).

the combined error over the whole 16 seconds and also over just the first 0.5 seconds. In the first plot, we can see that  $s$  does converge to the boundary layer as expected. The second plot shows more detail of the first 0.5 seconds. From this, we can see that  $s$  converges approximately as quickly as the second case in chapter 2. Figure 3.4 shows that combined error still stays within the boundary layer even with the disturbance. Finally, the state error, plotted in Figure 3.5,

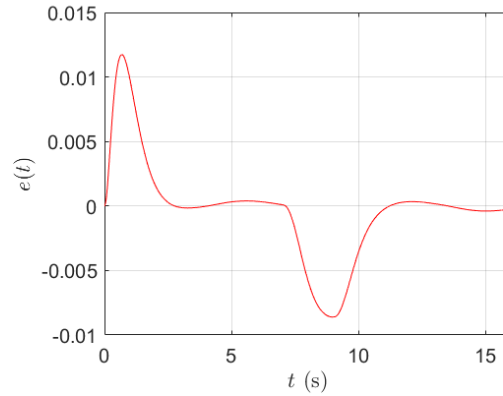


**Figure 3.5:** State error vs time.

does converge to its steady-state value near zero quite quickly but is affected by the disturbance. The steady-state errors as well as the minimum and maximum

**Table 3.2:** Combined and state errors.

$s_{ss}$	$e_{ss}$	$e_{\min}$	$e_{\max}$
$1.34 * 10^{-2}$	$3.91 * 10^{-4}$	-0.0086	0.0117

error listed in Table 3.2 are all similar to the results from the case 2 simulation in chapter 2 so our chapter 3 control law successfully reproduces the results from chapter 2 without manually tuning the boundary layer.

## Chapter 4. Adaptive Boundary Layer Sliding Mode Controller for a Plant with Unknown Parameters

### 4.1 Problem Statement

In this section, the work from the previous section is modified and extended to a plant with unknown parameters. A variable boundary layer is used in this section as well. The plant model is a  $n$ -th order system again described in the equation below as:

$$y^{(n)} + \sum_{i=1}^n \alpha_i f_i = bu + \delta. \quad (4.1)$$

The functions  $f_i$  for all  $i$  are known, but the system parameters  $b$  and  $\alpha_i$  for all  $i$  are unknown, so the following system models the actual plant with estimates of the unknown parameters:

$$y^{(n)} + \sum_{i=1}^n \hat{\alpha}_i f_i = \hat{b}u + \delta. \quad (4.2)$$

The equation parameters defined as:

$$h = 1/b, a_i = \frac{\alpha_i}{b}, d = -\delta/b \quad (4.3)$$

allow us to manipulate the equations (4.1) and (4.2) into the forms:

$$hy^{(n)} + \sum_{i=1}^n a_i f_i + d = u \quad (4.4)$$

$$\hat{h}y^{(n)} + \sum_{i=1}^n \hat{a}_i f_i + d = u. \quad (4.5)$$

Additionally, it is again assumed that the disturbance is bounded by some known value as:

$$|d| \leq D. \quad (4.6)$$

However, the bounds to the coefficients are no longer assumed to be known. The state error for the system is defined as

$$e = y - y_d, \quad (4.7)$$

where  $y_d$  is the desired output. The error dynamics are then

$$e^{(n-1)} = y^{(n-1)} - y_d^{(n-1)}. \quad (4.8)$$

This is then used to define the combined error as

$$s = e^{(n-1)} + \sum_{i=0}^{n-2} \binom{n-1}{i} \lambda^{n-i-1} e^{(i)}. \quad (4.9)$$

The above equation guarantees that if  $s$  vanishes, then the state error  $e$  exponentially approaches 0 for any positive  $\lambda$ . To obtain a more concise notation, the

reference value  $y_r^{(n)}$  is defined as:

$$y_r^{(n)} = y_d^{(n)} - \sum_{i=0}^{n-2} \binom{n-1}{i} \lambda^{n-i-1} e^{(i+1)}. \quad (4.10)$$

Taking the derivative of the combined error equation (4.9) and substituting the above equation into the result yields:

$$\dot{s} = y^{(n)} - y_r^{(n)}. \quad (4.11)$$

## 4.2 Error Behavior

*Lemma:* If the control law

$$u = \hat{h}y_r^{(n)} - k\text{sat}\left(\frac{s}{\phi_s}\right) + \sum_{i=1}^n \hat{a}_i f_i \quad (4.12)$$

with  $k > 0$  is applied to plant (4.4), then the closed loop response of the sliding variable  $s$  inside the boundary layer, in the absence of external disturbance, will be as follows:

$$\frac{h\phi_s}{k}\dot{s} + s = \rho, \quad (4.13)$$

where

$$\rho = \frac{\phi_s}{k}((\hat{h} - h)y_r^{(n)} + \sum_{i=1}^n (\hat{a}_i - a_i)f_i). \quad (4.14)$$

*Proof:* Solving equation (4.4) for  $y^{(n)}$  and substituting into equation (4.11) gives:

$$\dot{s} = \frac{1}{h} \left( u - \sum_{i=1}^n a_i f_i - d \right) - y_r^{(n)}. \quad (4.15)$$

Similar to the previous chapters, the control law would then ideally be chosen as:

$$u = h y_r^{(n)} - k \text{sat}\left(\frac{s}{\phi_s}\right) + \sum_{i=1}^n a_i f_i. \quad (4.16)$$

However, because the coefficients are unknown, the input is modified to:

$$u = \hat{h} y_r^{(n)} - k \text{sat}\left(\frac{s}{\phi_s}\right) + \sum_{i=1}^n \hat{a}_i f_i, \quad (4.17)$$

where  $k > 0$ . Again substitute equation (4.12) into equation (4.1) with  $d = 0$  to get:

$$h y^{(n)} + \sum_{i=1}^n a_i f_i = \hat{h} y_r^{(n)} - k \text{sat}\left(\frac{s}{\phi_s}\right) + \sum_{i=1}^n \hat{a}_i f_i. \quad (4.18)$$

Then add and subtract  $h y_r^{(n)}$  to get:

$$h y^{(n)} + \sum_{i=1}^n a_i f_i = \hat{h} y_r^{(n)} - h y_r^{(n)} + h y_r^{(n)} - k \text{sat}\left(\frac{s}{\phi_s}\right) + \sum_{i=1}^n \hat{a}_i f_i, \quad (4.19)$$

which leads to:

$$h y^{(n)} - h y_r^{(n)} + k \text{sat}\left(\frac{s}{\phi_s}\right) = \hat{h} y_r^{(n)} - h y_r^{(n)} + \sum_{i=1}^n \hat{a}_i f_i - \sum_{i=1}^n a_i f_i. \quad (4.20)$$

Thus, inside the boundary layer where  $\text{sat}(\frac{s}{\phi_s}) = \frac{s}{\phi_s}$ , the dynamics of the combined error is then:

$$\frac{h\phi_s}{k}\dot{s} + s = \rho, \quad (4.21)$$

where

$$\rho = \frac{\phi_s}{k}((\hat{h} - h)y_r^{(n)} + \sum_{i=1}^n (\hat{a}_i - a_i)f_i). \quad (4.22)$$

In fact,  $\rho$  is the effect on  $s$  of the error from using the parameter estimations instead of the real, unknown parameters.

*Lemma:* According to equation (4.21), if  $s$  is within the boundary layer, then  $\rho$  is small.

*Proof:* When  $s$  is within the boundary layer, the state errors are small. Thus, by equation (4.10), the reference value  $y_r^{(n)}$  is approximately equal to  $y_d^{(n)}$ . Then, by equation (4.11),  $\dot{s}$  must be small since  $y^{(n)} \approx y_d^{(n)}$  within the boundary layer. Therefore, by equation (4.21),  $\rho$  must be small because both  $s$  and  $\dot{s}$  are small.

### 4.3 Constant Boundary Layer

*Theorem:* Consider the system described by equation (4.4) and estimated by equation (4.5). The system parameters  $h$  and  $a_i$  for all  $i$  are unknown. The disturbance is bounded by (4.6). The control law is defined by equation (4.12) with  $k$  defined as:

$$k = D + \eta, \quad (4.23)$$

where  $\eta > 0$ . If the following adaptation laws

$$\dot{\hat{h}} = -\gamma_0^2 s y_r^{(n)} \quad (4.24)$$

$$\dot{\hat{a}}_i = -\gamma_i^2 s f_i \quad (4.25)$$

are used, then, as time passes,  $s$  approaches the boundary layer.

*Proof:* For the stability analysis, choose the Lyapunov function as:

$$V = \frac{1}{2}(hs^2 + (\frac{\hat{h} - h}{\gamma_0})^2 + \sum_{i=1}^n (\frac{\hat{a}_i - a_i}{\gamma_i})^2). \quad (4.26)$$

Take the derivative as:

$$\dot{V} = h s \dot{s} + \frac{\dot{\hat{h}}}{\gamma_0^2} (\hat{h} - h) + \sum_{i=1}^n \frac{\dot{\hat{a}}_i}{\gamma_i^2} (\hat{a}_i - a_i). \quad (4.27)$$

Using equation (4.15) for  $\dot{s}$ , we get

$$\dot{V} = h s (\frac{1}{h} (u - \sum_{i=1}^n a_i f_i - d) - y_r^{(n)}) + \frac{\dot{\hat{h}}}{\gamma_0^2} (\hat{h} - h) + \sum_{i=1}^n \frac{\dot{\hat{a}}_i}{\gamma_i^2} (\hat{a}_i - a_i). \quad (4.28)$$

Plug in the control law (4.12) and combine terms to get the following form:

$$\dot{V} = (\hat{h} - h) (s y_r^{(n)} + \frac{\dot{\hat{h}}}{\gamma_0^2}) + \sum_{i=1}^n (\hat{a}_i - a_i) (s f_i + \frac{\dot{\hat{a}}_i}{\gamma_i^2}) - s d - s k \text{sat}(\frac{s}{\phi_s}). \quad (4.29)$$

Then taking the adaptive laws as

$$\dot{\hat{h}} = -\gamma_0^2 s y_r^{(n)} \quad (4.30)$$

$$\dot{\hat{a}}_i = -\gamma_i^2 s f_i, \quad (4.31)$$

the Lyapunov derivative reduces to

$$\dot{V} = -s k \text{sat}\left(\frac{s}{\phi_s}\right) - s d. \quad (4.32)$$

Outside the boundary layer,  $\text{sat}(\frac{s}{\phi_s})$  is equivalent to  $\text{sgn}(s)$  and  $s \text{sgn}(s)$  is clearly  $|s|$  so we can rewrite this as

$$\dot{V} = -|s|k - s d. \quad (4.33)$$

We convert this to the inequality below:

$$\dot{V} \leq -|s|k + |s|D. \quad (4.34)$$

Choosing  $k = D + \eta$  where  $\eta > 0$  leads to

$$\dot{V} \leq -\eta|s|. \quad (4.35)$$

Hence,  $\dot{V}$  is always negative outside the boundary layer so it will decrease until  $s$  reaches the boundary layer.

## 4.4 Time-Varying Boundary Layer

### 4.4.1 Required Error Behavior for Varying Boundary Layer

*Lemma:* Consider the system described in section 4.1 with the controller described in section 4.3 modified to use a varying boundary layer. For  $s$  to approach the boundary layer when outside,  $s\dot{s} \leq (\dot{\phi}_s - \frac{\eta}{h})|s|$  proves this convergence.

*Proof:* Suppose  $s > \phi_s > 0$ . Then  $s$  clearly approaches  $\phi_s$  if and only if:

$$\frac{d}{dt}(s - \phi_s) \leq -\frac{\eta}{h} \quad (4.36)$$

where  $\eta > 0$ . Applying the derivative gives the equation:

$$\dot{s} - \dot{\phi}_s \leq -\frac{\eta}{h}, \quad (4.37)$$

which leads to:

$$\dot{s} \leq (\dot{\phi}_s - \frac{\eta}{h}). \quad (4.38)$$

But  $s > 0$ , so  $s = |s|$  and:

$$s\dot{s} \leq (\dot{\phi}_s - \frac{\eta}{h})|s|. \quad (4.39)$$

Alternatively, suppose  $s < -\phi_s < 0$ . Then clearly  $s$  approaches  $\phi_s$  if and only if:

$$\frac{d}{dt}(s - (-\phi_s)) \geq \frac{\eta}{h} \quad (4.40)$$

where  $\eta > 0$ . Applying the derivative gives the equation:

$$\dot{s} + \dot{\phi}_s \geq \frac{\eta}{h}, \quad (4.41)$$

which leads to:

$$\dot{s} \geq \left(\frac{\eta}{h} - \dot{\phi}_s\right). \quad (4.42)$$

But  $s < 0$  so  $s = -|s|$  and multiplying by  $s$  flips the inequality

$$s\dot{s} \leq \left(\dot{\phi}_s - \frac{\eta}{h}\right)|s|. \quad (4.43)$$

Hence,  $s$  converges to the boundary layer if  $s\dot{s} \leq \left(\dot{\phi}_s - \frac{\eta}{h}\right)|s|$ .

#### 4.4.2 Derivation of the Control Law

*Theorem:* Consider the system described by equation (4.4) and estimated by equation (4.5) where the system parameters  $h$  and  $a_i$  for all  $i$  are unknown, and the disturbance is bounded by (4.6). Using the adaptation laws (4.24) and (4.25) and the control law:

$$u = \hat{h}y_r^{(n)} - \bar{k}\text{sat}\left(\frac{s}{\phi_s}\right) + \sum_{i=1}^n \hat{a}_i f_i \quad (4.44)$$

with  $\bar{k} = k - \hat{h}\dot{\phi}$  where  $k = D + \eta$  for  $\eta > 0$ , then  $s$  approaches the time-varying boundary layer.

*Proof:* As the lemma in the previous section demonstrated, the goal is to show that  $s\dot{s} \leq \left(\dot{\phi}_s - \frac{\eta}{h}\right)|s|$  when outside the boundary layer. From equation

(4.11) with  $y^{(n)}$  from equation (4.4), the error dynamics becomes:

$$\dot{s} = \frac{1}{h} \left( u - \sum_{i=1}^n a_i f_i - d \right) - y_r^{(n)}. \quad (4.45)$$

Plugging in the value for  $u$  from equation (4.44) gives

$$\dot{s} = \frac{1}{h} \left( \hat{h} y_r^{(n)} - \bar{k} \text{sat} \left( \frac{s}{\phi_s} \right) + \sum_{i=1}^n \hat{a}_i f_i - \sum_{i=1}^n a_i f_i - d \right) - y_r^{(n)}. \quad (4.46)$$

Algebraically manipulating the equation allows us to write this as

$$\dot{s} = \frac{1}{h} \left( (\hat{h} - h) y_r^{(n)} + \sum_{i=1}^n (\hat{a}_i - a_i) f_i \right) - \frac{1}{h} \bar{k} \text{sat} \left( \frac{s}{\phi_s} \right) - \frac{1}{h} d. \quad (4.47)$$

We can plug in equation (4.14) with  $\bar{k}$  so

$$\dot{s} = \frac{\bar{k}}{\phi_s h} \rho - \frac{1}{h} \bar{k} \text{sat} \left( \frac{s}{\phi_s} \right) - \frac{1}{h} d. \quad (4.48)$$

Then, when there is no disturbance, assuming  $\bar{k} > 0$ , then the theorem from section 4.3 would guarantee that  $s$  does converge to the boundary layer. Then, by the second lemma from section 4.2,  $\rho$  must decrease to some small value. The above equation will then reduce to

$$\dot{s} \approx -\frac{1}{h} \bar{k} \text{sat} \left( \frac{s}{\phi_s} \right) - \frac{1}{h} d. \quad (4.49)$$

To get an equation of the correct form to be compared to equation (4.43) from the lemma, the above equation is multiplied by  $s$  and maximized to get an inequality:

$$s\dot{s} \leq -s\frac{1}{h}\bar{k}\text{sat}\left(\frac{s}{\phi_s}\right) + \frac{1}{h}|s|D. \quad (4.50)$$

Outside the boundary layer,  $\text{sat}\left(\frac{s}{\phi_s}\right) = \text{sgn}(s)$  and  $s\text{sgn}(s) = |s|$  so

$$s\dot{s} \leq -\frac{1}{h}\bar{k}|s| + \frac{1}{h}|s|D. \quad (4.51)$$

This can now be set equal to the equation (3.24) from the lemma:

$$\left(\dot{\phi}_s - \frac{\eta}{h}\right)|s| = -\frac{1}{h}\bar{k}|s| + \frac{1}{h}|s|D. \quad (4.52)$$

Dividing everything by  $|s|$  and isolating  $\bar{k}$  leads to

$$\bar{k} = \eta + D - h\dot{\phi}_s. \quad (4.53)$$

Using our estimate for  $h$  and plugging in  $k = D + \eta$ , we obtain

$$\bar{k} = k - \hat{h}\dot{\phi}_s. \quad (4.54)$$

Of important note, this analysis is dependent on the fact that  $\bar{k} > 0$ . Equation (4.49) is only valid if  $\rho$  does indeed decrease to a small value which, in section 4.2, was shown to be dependent on having a gain value greater than zero. Later,

using a lemma at the end of section 4.4.3, it is shown that, by the correct choice of  $\dot{\phi}_s$ ,  $\bar{k}$  is, in fact, positive.

#### 4.4.3 Derivation of the Boundary Layer Adaptation Law

*Theorem:* If  $\lambda_s$ , the rate of decay of  $s$ , is set equal to  $\lambda$ , the rate of decay of  $e$ , then the following boundary layer adaptation law is found:

$$\dot{\phi}_s = \frac{k}{\hat{h}} - \lambda\phi_s. \quad (4.55)$$

*Proof:* From equation (4.11) with  $y^{(n)}$  from equation (4.4), the error dynamics becomes:

$$\dot{s} = \frac{1}{h} \left( u - \sum_{i=1}^n a_i f_i - d \right) - y_r^{(n)}. \quad (4.56)$$

Plugging in the value for  $u$  from equation (4.44) gives

$$\dot{s} = \frac{1}{h} \left( \hat{h} y_r^{(n)} - \bar{k} \text{sat}\left(\frac{s}{\phi_s}\right) + \sum_{i=1}^n \hat{a}_i f_i - \sum_{i=1}^n a_i f_i - d \right) - y_r^{(n)}. \quad (4.57)$$

Inside the boundary layer, we can replace  $\text{sat}\left(\frac{s}{\phi_s}\right)$  with  $\frac{s}{\phi_s}$ :

$$\dot{s} = \frac{1}{h} \left( \hat{h} y_r^{(n)} - \bar{k} \frac{s}{\phi_s} + \sum_{i=1}^n \hat{a}_i f_i - \sum_{i=1}^n a_i f_i - d \right) - y_r^{(n)}. \quad (4.58)$$

Combining terms leads to

$$\dot{s} = \frac{1}{h} (\hat{h} - h) y_r^{(n)} + \frac{1}{h} \sum_{i=1}^n (\hat{a}_i - a_i) f_i - \frac{1}{h} \bar{k} \frac{s}{\phi_s} - \frac{1}{h} d \quad (4.59)$$

so we can substitute  $\rho$  from equation (4.14):

$$\dot{s} = \frac{\bar{k}}{\phi_s h} \rho - \frac{1}{h} \bar{k} \frac{s}{\phi_s} - \frac{1}{h} d. \quad (4.60)$$

Once again assuming that  $\bar{k} > 0$  we can say that  $\rho$  is small which reduces our equation to

$$\dot{s} \approx -\frac{1}{h} \bar{k} \frac{s}{\phi_s} - \frac{1}{h} d. \quad (4.61)$$

Estimating  $h$  as our  $\hat{h}$  we get

$$\dot{s} \approx -\frac{1}{\hat{h}} \bar{k} \frac{s}{\phi_s} - \frac{1}{\hat{h}} d. \quad (4.62)$$

The disturbance is bounded so  $s$  will be bounded as well, and the coefficient on the  $s$  term will drive the rate at which  $s$  decays. Thus, we set this rate  $\lambda_s$  equal to  $\lambda$ , the rate at which  $e$  decays:

$$\lambda_s = \frac{\bar{k}}{\hat{h} \phi_s} = \lambda. \quad (4.63)$$

Plugging in  $\bar{k}$  and solving for  $\dot{\phi}_s$  leads to the result:

$$\dot{\phi}_s = \frac{k}{\hat{h}} - \lambda \phi_s. \quad (4.64)$$

An important note is that the  $\hat{h}$  estimate must be hard-coded to stay above some minimum value greater than zero or  $\dot{\phi}_s$  could become unbounded. This can be justified based on the knowledge that  $h$  is known to be greater than zero.

*Lemma:* The adaptation law (4.64) for  $\phi_s$  ensures that  $\bar{k}$  is always positive.

*Proof:* We can now substitute our adaptation law (4.64) into equation (4.54) to get

$$\bar{k} = k - \hat{h}\left(\frac{k}{\hat{h}} - \lambda\phi_s\right). \quad (4.65)$$

The  $k$  terms cancel out so we are left with

$$\bar{k} = \hat{h}\lambda\phi_s. \quad (4.66)$$

Therefore, with this adaptive law,  $\bar{k}$  is indeed always greater than zero so the analysis in this section and section 4.4.2 are in fact valid.

## 4.5 Simulation

To demonstrate the results of this chapter, the control law was applied to a system in a simulation. The implementation of the simulation is shown below in Figure 4.1 with the relevant equations from this chapter. The same system and desired trajectory from section 2.4.1 was used with the same initial conditions and gain values listed in Table 4.1. The estimates of the parameters, that is  $\hat{h}$  and

**Table 4.1:** Control parameters and initial state for both cases.

$y(0)$	$\dot{y}(0)$	$\ddot{y}(0)$	$y^{(3)}(0)$	$\eta$	$\lambda$	$D$	$\phi_s(0)$
$\frac{25}{12}$	$-\frac{1}{3}$	-1.74	$\frac{1}{27}$	0.05	3	21	1

$\hat{a}_i$  for  $i = 1, \dots, n$ , are no longer constant for this chapter so they were initialized

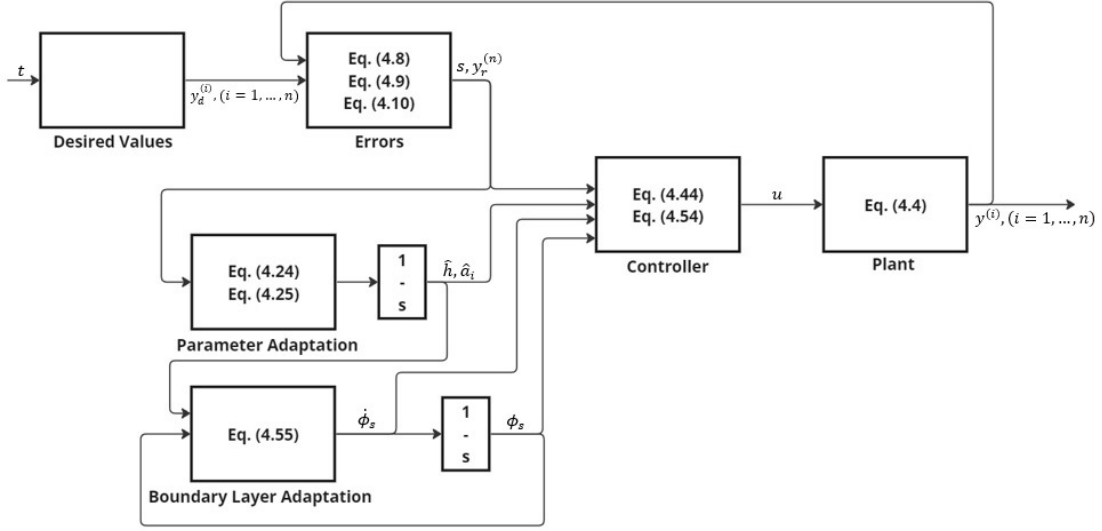


**Figure 4.1:** Block diagram of control law implementation.

at the values listed in Table 4.2. Two cases were simulated with differing initial conditions for the parameter estimates. Case 1 initialized the parameters at the values that were used in the chapters 2 and 3 for the constant parameter estimates. Case 2 initializes all five unknown parameters at 25. The  $\lambda_f$  parameter is still 0.25 as in the earlier chapter so the initial parameter estimates in case 2 are clearly all incorrect by orders of magnitude. The gains for the adaptive laws for the parameter estimates were set to  $\gamma_0 = 7$  and  $\gamma_i = 14$  for  $i = 1, \dots, 4$  after some tuning. In both cases,  $\hat{h}$  was hard-coded to be greater than or equal to 0.1.

Figure 4.2 shows that the controller does indeed provide tracking control in both cases despite not knowing the true plant parameters at all. Figure 4.3 shows the control input over time. The control input required is much higher in the first 0.5 seconds, so Figure 4.4 shows plots of the first 0.5 seconds and Figure

**Table 4.2:** Initial system parameter estimates and adaptation law gain values. (Case 1: initialized with nominal parameters. Case 2: initialized with randomly guessed parameters.)

	$\hat{h}(0)$	$\hat{a}_1(0)$	$\hat{a}_2(0)$	$\hat{a}_3(0)$	$\hat{a}_4(0)$	$\gamma_0$	$\gamma_1$	$\gamma_2$	$\gamma_3$	$\gamma_4$
Actual	1	$\lambda_f^4$	$4\lambda_f^3$	$6\lambda_f^2$	$4\lambda_f$					
Case 1	$\sqrt{0.9 * 1.4}$	$1.5\lambda_f^4$	$3\lambda_f^3$	$8\lambda_f^2$	$2\lambda_f$	7	14	14	14	14
Case 2	25	25	25	25	25	7	14	14	14	14

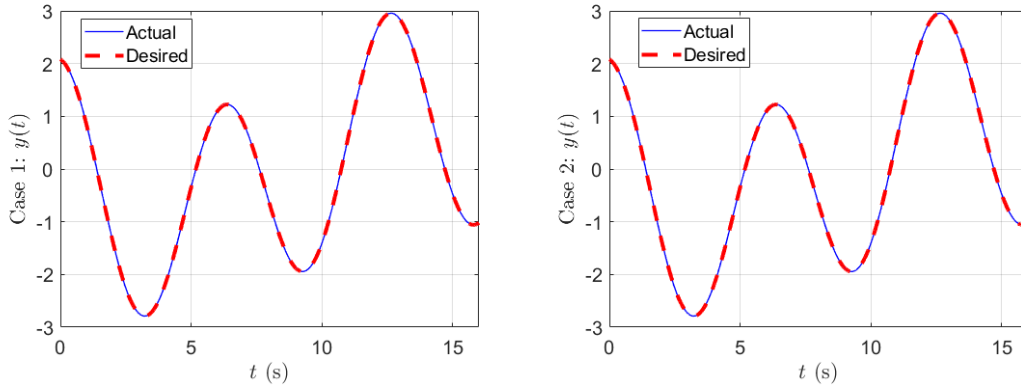


**Figure 4.2:** Actual and desired system state vs time.

4.5 shows more detailed plots of the input after the initial spike. Figure 4.4 shows that this control law does have much steeper requirements for the control input initially compared to the control laws from the previous chapters. This could be tuned with the  $\gamma_i$  parameters in the adaptation laws. The second case has a maximum absolute control input of about twice that of the first case so it can be gathered that a higher error in the initial estimate for the system parameters will lead to a higher control input. Figure 4.5 shows that the control input still attenuates the chatter very well due to our use of  $\text{sat}(\frac{s}{\phi_s})$  instead of  $\text{sgn}(s)$ . As

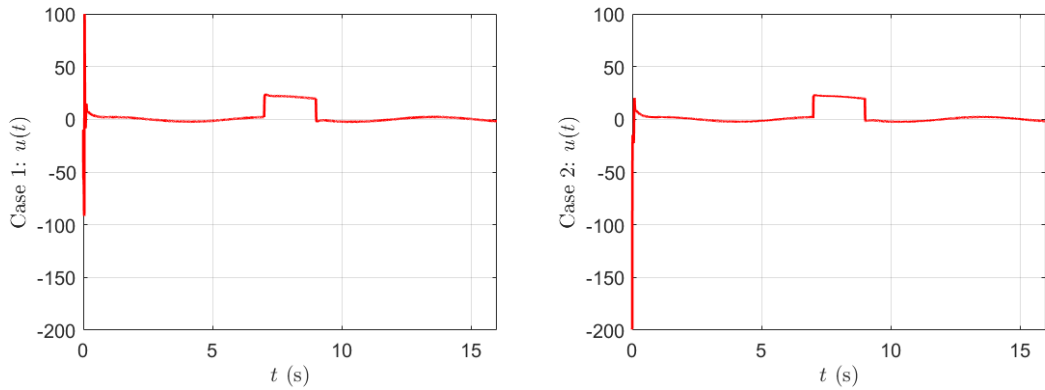


**Figure 4.3:** Control input vs time.

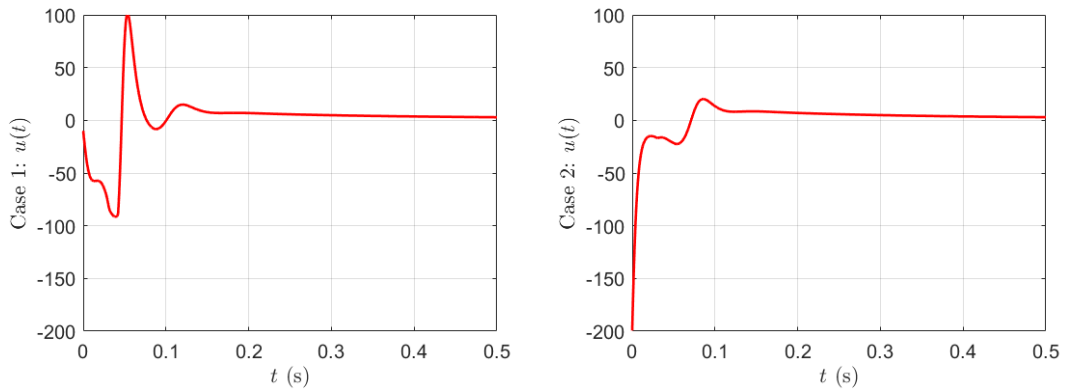


**Figure 4.4:** Control input vs time.

mentioned in chapter 2, an arbitrarily small boundary layer would not completely eliminate chatter, although it could still dampen the chatter significantly. The boundary layer used in our simulation is plotted in Figure 4.6. As can be seen, we initialized our boundary layer at  $\phi_s(0) = 1$ , but our adaptive law for the boundary layer increased it and decreased it as necessary to minimize the steady-state error while still attenuating chatter. Interestingly, the controller did a better job of eliminating the chatter in the first case. Additional work should be done

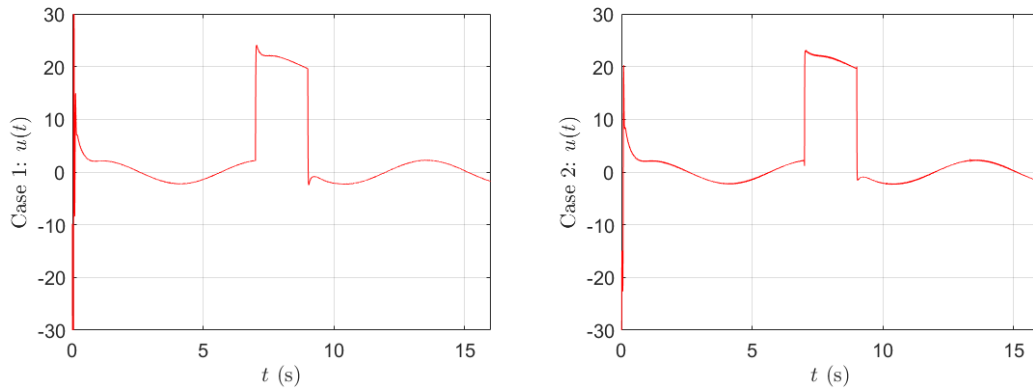


**Figure 4.5:** Control input vs time.

to determine why this is the case. Figure 4.6 also shows that  $s$  does converge

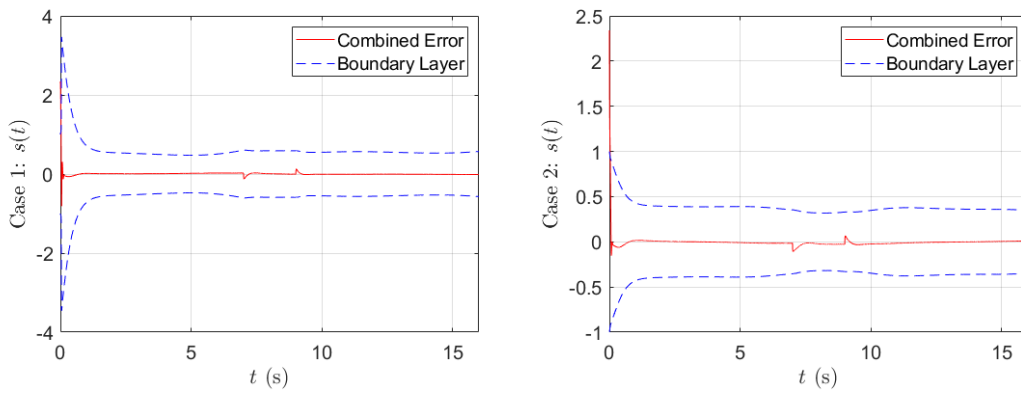


**Figure 4.6:** Combined error vs time.

to the boundary layer as expected. Interestingly,  $s$  appears to be less affected by the disturbance as it was in chapters 2 and 3. There is only a small spike when the disturbance is added and removed. The state error, plotted in Figure 4.7, converges towards zero quite quickly as well with the disturbance only mildly affecting it. The error, in fact, is actually less affected than it was in chapters 2 and 3 because  $s$  was less affected. As can be seen in Figure 4.8, the residual is

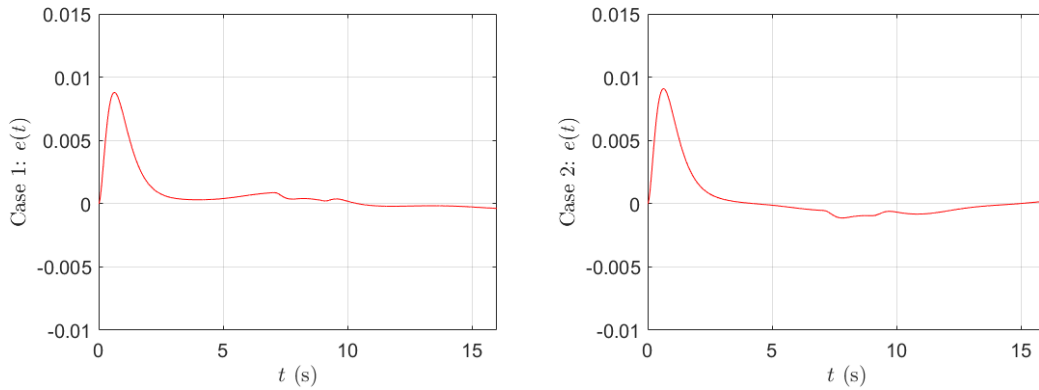


**Figure 4.7:** State error vs time.

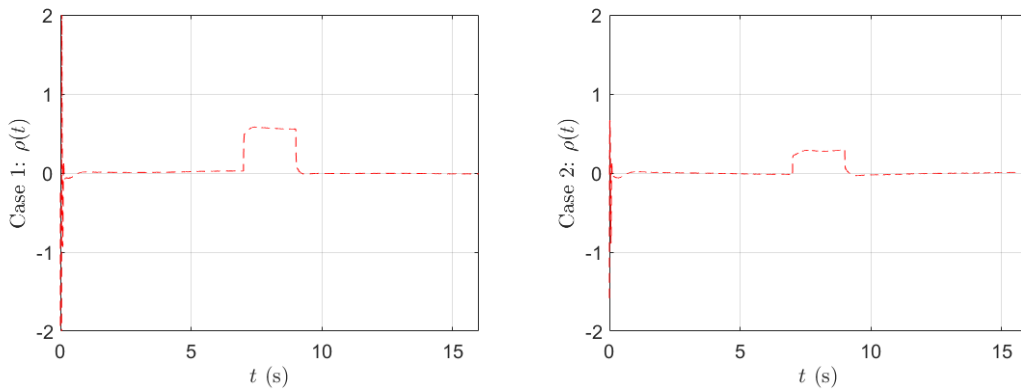


**Figure 4.8:** Residual rho vs time.

very small after  $s$  converges to the boundary layer and stays small except when the large disturbance is applied. The steady-state errors as well as the minimum and maximum errors are listed in Table 4.3 below. Case 2 has steady-state values approximately three times the steady state values in case 1 for both  $s$  and  $e$ . The minimum and maximum errors are also slightly larger. However, initial errors for the unknown parameter estimates were orders of magnitude higher in the second case, so such a small difference in the steady-state errors still demonstrates that

**Table 4.3:** Combined and state errors.

	$s_{ss}$	$e_{ss}$	$e_{\min}$	$e_{\max}$
Case 1	$0.24 * 10^{-2}$	$0.66 * 10^{-4}$	-0.0004	0.0088
Case 2	$1.52 * 10^{-2}$	$5.28 * 10^{-4}$	-0.0019	0.0091

our control law works successfully even with highly inaccurate initial guesses for the parameters. Furthermore, the difference between the steady-state errors of the two cases was seen to effectively vanish after about 500 seconds in longer simulations. The steady-state errors are very similar to the errors in Table 3.2, so this control method provides good tracking control comparable to the control method in chapter 3 without requiring bounds for the parameters.

## Chapter 5. Conclusion

The proofs developed in this paper show the potential of using an adaptive SMC with an adaptive boundary layer to control an arbitrary  $n$ th-order plant. The simulations in sections 2.4, 3.4, and 4.5 demonstrate the value of this approach when applied to a 4th-order system with unknown parameters. In the proofs and simulations in chapter 2 and chapter 3, an SMC with a constant and adaptive boundary layer, respectively, were applied to a plant showing the benefit of using an adaptive boundary layer instead of a constant boundary layer. In chapter 4, a boundary layer adaptation law was derived that can be applied to a plant with unknown parameters, together with an SMC that uses adaptation laws to compensate for the unknown parameters. Table 5.1 summarizes the results from all three control law simulations. The steady-state  $s$  and  $e$  for the chapter 3 simulation is quite similar to that of the second case from chapter 2 where the boundary layer was tuned to  $\phi_s = 0.3$  manually. The minimum and maximum error are similar as well, so the adaptive boundary layer is superior to the constant boundary layer, as it did not require the same tuning but gave comparable results. The results from chapter 4 show somewhat similar errors as chapter 2. As for the difference between the errors in case 1 and 2 of chapter 4, it does appear the differences effectively vanish eventually, but only after about 500

**Table 5.1:** SMC methods: combined and state errors.

	$s_{ss}$	$e_{ss}$	$e_{\min}$	$e_{\max}$
Chapter 2: $\phi_s = 0.05$	$1.50 * 10^{-2}$	$0.74 * 10^{-4}$	-0.0016	0.0117
Chapter 2: $\phi_s = 0.3$	$1.38 * 10^{-2}$	$4.20 * 10^{-4}$	-0.0098	0.0117
Chapter 3: $\phi_s(0) = 1$	$1.34 * 10^{-2}$	$3.91 * 10^{-4}$	-0.0086	0.0117
Chapter 4: Nominal Parameter Estimates	$0.24 * 10^{-2}$	$0.66 * 10^{-4}$	-0.0004	0.0088
Chapter 4: Random Parameter Estimates	$1.52 * 10^{-2}$	$5.28 * 10^{-4}$	-0.0019	0.0091

seconds. Thus, the simulations in chapter 4 suggest a small sacrifice in transient error behavior as compared to chapters 2 and 3. The primary sacrifice, though, is seen in the control input during the initial transient phase. As mentioned in section 4.5.1, the simulation in chapter 4 had noticeably higher control input values in the transient behavior. In practice, the control laws of chapter 3 and chapter 4 would be most useful in different situations, as listed in Table 5.2. If a set of nominal parameters and well-defined bounds for the parameter error are known, the control method of chapter 3 would be desirable due to its lower initial control input values during the transient phase. Without the nominal parameters and well-defined bounds for the parameter error, the chapter 3 method would not be implementable, but the method from chapter 4 could still be implemented with nearly as good results. Ultimately, the simulations demonstrated that the control method from chapter 4 provides adequate tracking control with steady-state

**Table 5.2:** SMC methods: benefits and drawbacks.

	Chapter 2	Chapter 3	Chapter 4
Boundary Layer (BL)	Constant	Adaptive	Adaptive
System Parameters (SP)	Known Bounds	Known Bounds	Unknown
BL Tuning	Manual	Adaptive	Adaptive
Chattering	Good BL Tuning: Eliminated Bad BL Tuning: Exists	Automatically Eliminated	Automatically Eliminated
Steady-State Error	Good BL Tuning: Good Bad BL Tuning: Better	Better	Best
Initial Control Effort	Low	Low	High
Suggested Use	Do Not Use	Known SP Bounds	Unknown SP

behavior comparable to the control method in chapter 3 that relies on known bounds of uncertain parameters.

## References

- [1] Christopher Edwards and Sarah K Spurgeon. *Sliding Mode Control: Theory And Applications*. CRC Press, Milton, 1 edition, 1998.
- [2] K.D. Young, V.I. Utkin, and U. Ozguner. A control engineer’s guide to sliding mode control. *IEEE transactions on control systems technology*, 7(3):328–342, 1999.
- [3] I. Boiko, L. Fridman, A. Pisano, and E. Usai. Analysis of chattering in systems with second-order sliding modes. *IEEE transactions on automatic control*, 52(11):2085–2102, 2007.
- [4] I. Boiko and L. Fridman. Analysis of chattering in continuous sliding-mode controllers. *IEEE Transactions on Automatic Control*, 50(9):1442–1446, 2005.
- [5] Jiyu Xia and Huimin Ouyang. Chattering free sliding mode controller design for underactuated tower cranes with uncertain disturbance. *IEEE transactions on industrial electronics (1982)*, 71(5):1–12, 2024.
- [6] Hoon Lee and Vadim I. Utkin. Chattering suppression methods in sliding mode control systems. *Annual reviews in control*, 31(2):179–188, 2007.
- [7] Vadim Utkin and Hoon Lee. Chattering problem in sliding mode control systems. *Analysis and Design of Hybrid Systems 2006*, 39(5):1–1, 2006.
- [8] Lei Guo, Han Zhao, and Yuan Song. A nearly optimal chattering reduction method of sliding mode control with an application to a two-wheeled mobile robot. *arXiv (Cornell University)*, 2021.
- [9] Carlos Arturo Martínez-Fuentes, Ulises Pérez-Ventura, and Leonid Fridman. Chattering analysis for lipschitz continuous sliding-mode controllers. *International journal of robust and nonlinear control*, 31(9):3779–3794, 2021.
- [10] Avi Hanan, Arie Levant, and Adam Jbara. Low-chattering discretization of homogeneous differentiators. *IEEE transactions on automatic control*, 67(6):2946–2956, 2022.

- [11] J.-J. E. (Jean-Jacques E.) Slotine and Weiping Li. *Applied nonlinear control*. Prentice Hall, Englewood Cliffs, N.J, 1991.
- [12] J. A. BURTON and A. S. I. ZINOBER. Continuous approximation of variable structure control. *International journal of systems science*, 17(6):875–885, 1986.
- [13] Prasheel V. Suryawanshi, Pramod D. Shendge, and Shrivijay B. Phadke. A boundary layer sliding mode control design for chatter reduction using uncertainty and disturbance estimator. *International journal of dynamics and control*, 4(4):456–465, 2016.
- [14] Tiffany Lodge. Adaptive boundary layer sliding mode control for multi-input-multi-output systems, 2023.
- [15] Lei Wan, Guofang Chen, Mingwei Sheng, Yinghao Zhang, and Ziyang Zhang. Adaptive chattering-free terminal sliding-mode control for full-order nonlinear system with unknown disturbances and model uncertainties. *International journal of advanced robotic systems*, 17(3):172988142092529–, 2020.
- [16] Yufei Liang, Dong Zhang, Guodong Li, and Tao Wu. Adaptive chattering-free pid sliding mode control for tracking problem of uncertain dynamical systems. *Electronics (Basel)*, 11(21):3499–, 2022.
- [17] Vadim Utkin, Alex Poznyak, Yury V Orlov, and Andrey Polyakov. High-order sliding mode control. In *Road Map for Sliding Mode Control Design*, SpringerBriefs in Mathematics, pages 83–89. Springer International Publishing AG, Switzerland, 2020.
- [18] Michael Defoort, Thierry Floquet, Annemarie Kokosy, and Wilfrid Perruquetti. A novel higher order sliding mode control scheme. *Systems & control letters*, 58(2):102–108, 2009.
- [19] Hussein U. Suleiman, Muhammed B. Murazu, Tahir A. Zarma, Ahmed T. Salawudeen, Sadiq Thomas, and Ahmadu A. Galadima. Methods of chattering reduction in sliding mode control: A case study of ball and plate system. In *2018 IEEE 7th International Conference on Adaptive Science & Technology (ICAST)*, volume 2018-, pages 1–8. IEEE, 2018.

- [20] C. Arturo Martínez-Fuentes, Jaime A. Moreno, and Leonid Fridman. Anti-chattering strategy using twisting controller. *IFAC-PapersOnLine*, 51(13):384–389, 2018.
- [21] Junxiao Wang, Shihua Li, Jun Yang, Bin Wu, and Qi Li. Extended state observer-based sliding mode control for pwm-based dc–dc buck power converter systems with mismatched disturbances. *IET control theory & applications*, 9(4):579–586, 2015.
- [22] Ryan Mathewson and Farbod Fahimi. Nonlinear adaptive sliding mode control with application to quadcopters. *Nonlinear engineering*, 12(1):115–25, 2023.